UNIVERSITAT POLITÈCNICA DE CATALUNYA
BARCELONATECH

MASTER THESIS

Power Efficiency Enhancement of Transmitters using Adaptive Envelope Tracking and Shaping Techniques for Small Payload Space Applications

Hafiz Faisal Rasool

SUPERVISED BY

Pere Lluís Gilabert Pinal

Gabriel Montoro Lopez

Master in Aerospace Science and Technology

UNIVERISTAT POLITÈCNICA DE CATALUNYA

September 2015

Page intentionally left blank

Acknowledgments

In the name of God, the most Gracious, the most Merciful.

First of all, I want to express my sincerest gratitude towards my project supervisor, Mr. Pere L. Gilabert who has guided me throughout the course of this work with his tremendous amount of support and knowledge. He has helped me understand and resolve every issue with extreme patience. I would also like to thank my co-supervisor Mr. Gabriel Montoro who has been really helpful with his feedback on every step of the way during my work at Signals Theory and Communications (TSC) Lab, UPC.

Studying at EETAC has been a magnificent opportunity for me and I want to thank all my fellows at MAST who have made this experience even more rewarding in terms of knowledge and growth. I would want to thank everyone at my organization, SUPARCO, who has supported me during my studies at UPC.

My acknowledgement extends to all of my friends especially Minhaj Usmani who have stood by me throughout my life and I am indebted to every one of them.

Ultimately, everything that I have achieved in my life is due to unconditional love and relentless support of my parents and I want to thank everyone in my family for believing in me especially my father who has helped me grow into the person I am and urged me to always take that one more step.

Page intentionally left blank

Abstract

With the rise of modular system architecture for distributed satellite systems with multiple small payloads instead of conventional larger spacecrafts, the efficient characterization of power budget and available power constraints become even more vital. In order to establish high data rate downlink communications in small satellite applications, use of highly efficient, non-conventional power amplification techniques is going to be a key factor in future communication systems. The concept of having small, less power consuming and high data rate transmission system extends to vast number of applications like light weight Unmanned Aerial Vehicle (UAV) and hand-held communication modules etc.

The idea is to study and develop an adaptive envelope tracking technique which should be able to dynamically supply power to Radiofrequency power amplifier. Consequently, an optimal control over system power consumption leads to enhanced efficiency. The amplifiers intended for such systems exhibit nonlinear behavior when it comes to operating at maximum output power and cause distortion in adjacent bands. Introducing a power supply modulation block in combination with digital linearization techniques such as DPD offers considerable improvement.

This thesis tests a dynamic power supply adaptive shaping technique for LTE signals. In comparison to conventional fixed supply RF PAs, Envelope Tracking PA has resulted in improved linearity at the output as well as reduced unwanted power leakage into adjacent frequency channels. By imposing an isogain trajectory trough the shaping function, we can optimize the available power for high data rate communications while keeping the intermodulation distortion at acceptable levels by considering a tradeoff between efficiency and computational load.

Page intentionally left blank

Contents

Acknowledgments **2**
Abstract **4**
List of Tables **8**
List of Figures **9**
Glossary **10**
1 Introduction **12**
1.1 Motivation 12
1.2 Objective and Methodology 14
1.3 Thesis Outline 15
2 High Efficiency PAs and Linearity **16**
2.1 Problem Definition 16
2.2 Power Added Efficiency 16
2.3 Signal Characteristics 17
2.4 PA Basics 18
2.4.1 Nonlinear Memoryless Model 20
2.4.2 Memory Effect on PA Models 21
2.5 Performance Characterization 21
2.6 PA Model Estimation 23
3 Envelope Tracking and Shaping for Power Amplifiers **26**
3.1 Fundamentals of Envelope Tracking 26
3.2 ET System Architecture 28
3.3 Efficiency Vs Linearity for ET PAs 29
3.4 Performance Enhancement of RF PA 29
3.4.1 Digital Pre-Distortion 30
3.5 Envelope Shaping Function 32
3.5.1 Adaptive Iso-Gain Shaping Model 33
3.6 Manual Envelope Shaping and Spline Model 34
3.6.1 Linear Splines 35
3.6.2 Quadratic Splines 37
3.6.3 Cubic Splines 38
3.7 Manual Isogain Shaping 41
3.7.1 Isogain Line or Targeted Gain 42
4 Experimental Setup **44**

4.1 Device-Under-Test Setup 44
4.2 DUT Test Scenarios 45
4.2.1 Dynamic Supply with No Shaping 47
4.2.2 Adaptive Shaping 48
4.2.3 Adaptive Shaping with IQ DPD 50
4.3 Performance Comparison 53
4.3.1 Manual Shaping vs Adaptive Shaping 53
4.3.2 Spline Interpolated Manual Shaping Model 54
5 Conclusion 59
Bibliography 61

List of Tables

Table 2-1: Comparison of PAPR values with PA Efficiency 18
Table 2-2: System Order and NMSE 24
Table 3-1: Spline Model Estimation performance for sinusoidal test function 40
Table 4-1: Test Parameters 46
Table 4-2: Performance Comparison 53
Table 4-3: Manual vs Adaptive Shaping 54
Table 4-4: Input Envelope and Power Supply 56

List of Figures

Figure 1-1: Distributed Satellite Systems 13
Figure 2-1: Generic Block Diagram of a Wireless Communication System 19
Figure 2-2: PA Block 19
Figure 2-3: Input-Output Response curves for an Ideal and Real PA 20
Figure 2-4: Linear Output and Intermodulation Products 22
Figure 2-5: AM-AM Response of PA 23
Figure 2-6: Memoryless PA Model for 5 MHz LTE Signal 25
Figure 2-7: PA Model with 2 Memory Taps for 5 MHz LTE Signal 25
Figure 3-1: Power Supply Architecture 27
Figure 3-2: Envelope and Transmitted Power 27
Figure 3-3: ET PA Block Diagram 28
Figure 3-4: DPD Principle with Resultant Signal Spectrum 30
Figure 3-5: Device Efficiency and Output Power 31
Figure 3-6: Efficiency and Gain Vs System Output (Optimum Efficiency Shaping) 32
Figure 3-7: ET PA with Envelope Shaping Block 33
Figure 3-8: Spline Fitting 35
Figure 3-9: Linear Splines 36
Figure 3-10: Linear Spline Interpolated Sine function 36
Figure 3-11: Quadratic Spline Interpolated Sine function 38
Figure 3-12: Cubic Spline Interpolated Sine function 40
Figure 3-13: Measured DC Supply and Back-off for LTE 5MHz signal 41
Figure 3-14: Gain vs Output Power for LTE 5MHz signal 42
Figure 3-15: Gain vs Input Power (Targeted Gain = 35.2667dB) 43
Figure 3-16: Gain vs Input Power (Targeted Gain = 39.267dB) 43
Figure 4-1: Block Diagram of Testbed 45
Figure 4-2: Instruments Layout 45
Figure 4-3: 5 MHz Input Signal Spectra 46
Figure 4-4: AM-AM Curve for Dynamic Supply Model without shaping function 47
Figure 4-5: AM-PM Response for Dynamic Supply Model with shaping function 47
Figure 4-6: RF Output Spectrum for Dynamic Supply Model without shaping function 48
Figure 4-7: AM-AM Curve for Adaptive Shaping Model 49
Figure 4-8: AM-PM Response for Adaptive Shaping Model 49
Figure 4-9: RF Output Spectrum for Adaptive Shaping Model 50
Figure 4-10: Shaping Function curve for Adaptive Shaping Model 50
Figure 4-11: AM-AM Response for AS + IQ DPD 51
Figure 4-12: AM-PM Response for AS + IQ DPD 51
Figure 4-13: RF Output Spectrum for AS + IQ DPD 52
Figure 4-14: Shaping Function curve for AS + IQ DPD 52
Figure 4-15: Gain vs Input Power (Targeted Gain = 35.2667dB) 55
Figure 4-16: Gain vs Input Power (Targeted Gain = 39.267dB) 55
Figure 4-17: Shaping Model (35.2667dB Gain) 57
Figure 4-18: Shaping Model (39.267dB Gain) 57

Glossary

ACPR	**ACPR Adjacent Channel Power Ratio**
ACEPR	**Adjacent Channel Error Power Ratio**
ACLR	**Adjacent Channel Leakage Ratio**
AM	**Amplitude Modulation**
DC	**Direct Current**
DE	**Drain Efficiency**
DPD	**Digital Predistortion**
EA	**Envelope Amplifier**
FPGA	**Field-programmable Gate Array**
IQ	**In-phase/Quadrature**
LTE	**Long-Term Evolution**
NMSE	**Normalized Mean Squared Error**
PA	**Power Amplifier**
PAE	**Power Added Efficiency**
PAPR	**Peak-to-Average Power Ratio**
PM	**Phase Modulation**
RF	**Radiofrequency**
WCDMA	**Wideband Code Division Multiple Access**

Page intentionally left blank

1 Introduction

This thesis discourses the need and methodology to enhance power efficiency of modern communication modules which range from handheld devices to small payload space applications. Over the years, performance of radio communication standards has been improved with the emergence next out of the box idea until the system saturates its resources such as available power and RF spectrum. Therefore, it is vital to achieve optimal resource utilization by exploiting the characteristics of key components like power amplifier.

In a typical RF communication system, PA is the most power hungry component, and the fact that it also presents a non-linear behavior for different operating regions warrants thorough study. When it comes to PAE of modern communication standards (Wi-Fi, LTE), the conventional fixed supply PAs limit the system performance because for a rapidly varying input signal with high *'Peak-to-Average Power Ratio'* (PAPR) values, a lot of power is wasted in amplifying signals with low input power. A significant drop in PAE from GSM (65 %) to LTE (30 %) highlights the challenge [1]. This objective of the thesis is to study techniques for improving PAE by and test an algorithm on a *'Device-Under-Test'* (DUT) to understand how a more dynamic control over power supply to a PA offers improved resource utilization. The idea lends its applications to power constrained nanosatellites, where the need to use less power to transfer maximum amount of information is ever increasing.

1.1 Motivation

The importance of understanding and exploring the possibility to improve system performance on component level is justified by the sheer volume of communication industry. The applications of an efficient communication system range from mobile devices to completely autonomous satellites. Telecommunications industry amasses a volume of approximately $5 Trillion worldwide. In 2013, mobile industry contributed to 3.6 % global GDP and this figure is expected to rise to 5.1 % in 2020. This segment of telecommunication industry has seen the most dramatic rise in just over 10 years. In 2003, there were approximately one billion unique subscribers and this has risen to 3.4 billion unique subscribers worldwide in 2013 with 6.9 billion SIM connections [2]. Satellite communication industry makes up for more than 60 % of the $195 Billion global satellite business. More than 50 % of operating satellites are primarily for communication and more than 40 % of these satellites are used for commercial communication systems and services providing civilian

users with satellite broadcasting, telephony, navigation and location based services. An increase in telecommunication industry revenues by 7 % in 2013 emphasizes that the demand is still increasing and further research and development of means is mandated [3].

From space applications perspective, clustered or distributed satellite systems with modular designs instead of huge single unit missions are a way forward. As a spacecraft is divided into different small satellites flying in close proximity formations, the power resources become fewer, whereas the demand of instantaneous handshakes and huge chunks of data exchange between multiple systems rises. The problem can be addressed with the use of extremely efficient PA for communication system which makes use of dynamic power supply schemes based on the kind of information being exchanged. The system configuration is illustrated in the fig. 1-1 [4].

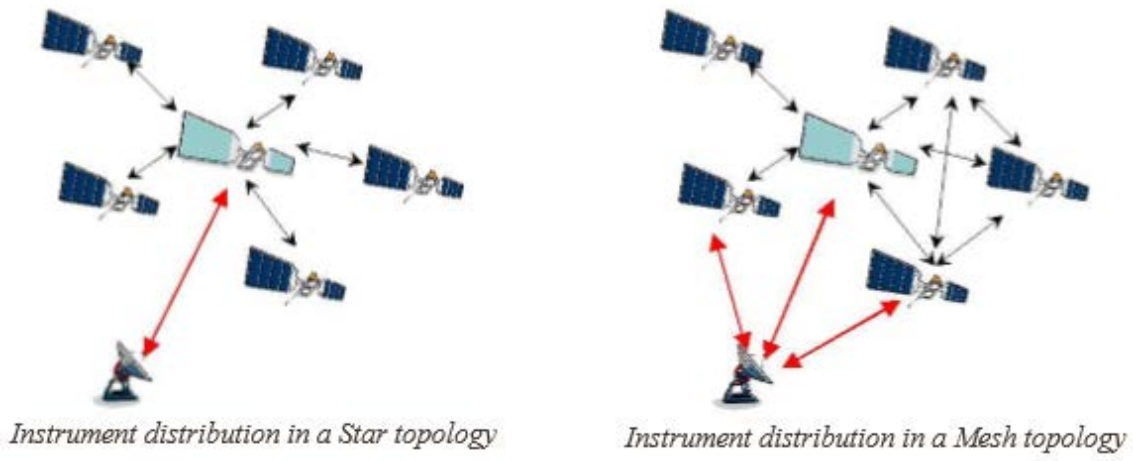

Figure 1-1: Distributed Satellite Systems

With the advent of high data rate communication standards, strict linearity and bandwidth requirements have been put in place for infrastructure and mobile applications.

PA is the most power consuming component in the transmitter chain with value of power used by PA alone rising up to 85 % [5], whereas the PAE is relatively low (< 50 %) for non-infrastructure applications. Traditional fixed supply PAs can be replaced with Envelope Tracking linear RF PA with a supply modulating circuitry to increase performance. Higher throughput gave rise to complex digital modulation schemes such as quadrature amplitude modulation (QAM) and orthogonal frequency division multiplexing (OFDM). However, the

resultant signals have higher PAPR values, which have increased from 0 dB (GSM) to more than 10 dB for LTE [1]. Strong peaks of input signal as compared to moderate average power levels cause saturation at the output. Therefore, PAs need to operate below their maximum output power to avoid this phenomenon but the result is decreased efficiency. Use of a dynamic supply modulation technique ensures that PA operates in compression (high efficiency) for a wider range of input signals. The added advantage of ET PAs over fixed supply PA is considerably less heat dissipation improving component life time.

The statistics of high PAPR signals suggest that ET PAs spend more time operating at lower supply voltages whereas the higher instantaneous peaks are relatively few. Therefore, ET amplifiers are matched to be optimized for targeted high PAPR signals because generally RF PAs are configured to operate below high efficiency region in order to avoid compression caused by high peak values of input signal.

1.2 Objective and Methodology

The aim of this thesis is to study and comprehend the fundamentals of power amplification for RF communication. By understanding how the previous transmission standards evolved into newer high speed and efficient techniques, it is established that PAE is the figure of merit that primarily defines a system's performance. Identification of the problem leads to study of an alternative strategy to conventional fixed supply PAs for high PAPR applications. A system where dynamically varying power supply is modulated based on the input power of baseband signal is implemented. Instead of using a constant supply voltage for PA, where a sizeable amount of power was lost in heat dissipation, PAE is improved by introducing an input envelope tracking and shaping function which controls an *Envelope Amplifier* or supply modulator. Efficiency however, is not only dependent on RF PA and envelope amplifier but the computational complexity of linearization algorithm which is used to compensate for nonlinear distortion appearing at RF PA output. Therefore, an efficient linearization technique also plays a vital role towards system performance. ET and shaping block is used to perform magnitude calculation of complex digital signal, and an instantaneous power supply voltage can be chosen. Characterization of PA behavior over a range of supply values is performed using gain vs output power. It then becomes convenient to target either a fixed output gain at the cost of efficiency with upside being smaller distortion in PA output. A tradeoff can be made between linearity and efficiency by also understanding optimum efficiency shaping in which the PA is made to operate in compression over a wide range of

output power values. Another aspect of the work is to study *Spline* interpolation that is used for mapping required instantaneous power supply level against an envelope sample value. Following step-wise approach is adopted:

- Study of PA performance characteristics and behavioral modelling
- Envelope Tracking and Shaping function simulation with Spline Interpolation
- System level tests of algorithm with DUT and analysis of results

1.3 Thesis Outline

The work presented in the thesis follows a modular approach starting with PA efficiency improvement as objective, establishing envelope tracking PAs as a viable alternative it concludes with experimental setup and simulation results using a real time test-bed.

Chapter 2 includes problem identification, an overview of basics of the PA, performance characteristics and figures of merit. Keeping in view the objective, a tradeoff between linearity and system efficiency is discussed for acceptable performance standards.

Chapter 3 develops the theory of Envelope Tracking amplifiers, envelope shaping function and use of dynamic power supply for PA to enhance performance. Iso-gain characteristics with system level block diagram and architecture of close-loop envelope tracking and shaping functional blocks. Spline Interpolation theory and an algorithm to identify a cubic spline model concludes the chapter.

Chapter 4 introduces hardware test-bed, experimental results with adaptive and non-adaptive envelope shaping. Digital Pre-Distortion technique for AM-PM distortion reduction is introduced in RF signal path to PA and results are analyzed.

Chapter 5 provides a conclusion of thesis summarizing the objective and outcome of the project developed.

2 High Efficiency PAs and Linearity

Power amplifiers are the most critical block in a transmission chain with the requirement to produce high power RF output by amplifying an input RF signal with the use of DC power supply voltage. The amplified RF signal is then used for a reliable information transfer between user equipment (UE) and base stations (BTSs) in mobile communication applications. The available system resources such as power and bandwidth are limited and strictly monitored. Infrastructure based applications such as BTS usually have more power at their disposal but power utilization becomes extremely critical for handheld communication modules. Since RF PAs support most of the global communication standards like GSM, WCDMA and LTE, it is critical to understand the relation between power consumption requirements and efficiency.

2.1 Problem Definition

Generally, in communication systems' evolution the emphasis has been on high data rate and maximum spectrum utilization. Emerging standards such as WCDMA, high speed packet access (HSPA) and long term evolution (LTE) use modulated signals with a rapidly varying envelope. A performance metric is introduced to define signal characteristics known as PAPR. It compares peak output value to time-average output power value. High PAPR meant that PAs transmitted peak power on relatively fewer occasions and operated at low output powers. For fixed supply RF PAs, it means that a minor portion of DC power supply is used for amplification of input signal and rest is dissipated in heat losses. Therefore, efficiency drops because PAs exhibit maximum performance when operated in compression. An alternative approach to fixed supply PA is to dynamically vary DC power supply keeping the operation of PA in high efficiency region. An improved PAE is the objective for considering the above mentioned modulated DC supply approach.

2.2 Power Added Efficiency

Ideally, all DC power consumed by a PA should appear at the output which is not the case for real systems. For PAs, there are two parameters called *Drain Efficiency* (DE) and *Power Added Efficiency* (PAE) which characterize an amplifier. DE is the ratio of output power to the consumed DC power supply.

$$DE = \frac{P_{out}}{P_{DC}} \times 100\ \% \tag{2.1}$$

P_{out} is transmitted RF power at the output and P_{DC} is DC power consumed for amplification. DE defines how much of DC power is converted into output power but it does not provide a measure of input RF power which is fed to PA for amplification. For a single stage RF PA, the incident RF power in input signal is considerable. However DE is an important quantity when the efficiency based on an Envelope Tracking PA and supply modulator circuitry is considered.

PAE becomes a comprehensive figure of merit to define RF PA performance because it is measure of power conversion efficiency, taking into account the amount of RF power in the input signal as well.

$$PAE = \frac{P_{out} - P_{in}}{P_{DC}} \times 100\ \% \tag{2.2}$$

P_{in} is input RF signal power. Eq. 2.2 shows that a PA with higher PAE value has a longer operation time from a power constrained application's perspective.

2.3 Signal Characteristics

Based on the objective of finding an efficient RF power amplification scheme, the need to understand modern signals which are used for high data rate transmission standards is paramount. Complex, multicarrier digital modulation schemes provide high data rates and the input signal characteristics have changed but high level system requirements are constrained by physical system limits i.e. an RF PA usually defines performance limits of a system. There is a demand of linearity from RF PA even at peak output powers keeping the distortion limited, but a PA optimized for high linearity drops in efficiency except for signal peaks which are fewer in high PAPR signals. Therefore, Linearity and efficiency tradeoff requires understanding of shape of the signal.

Crest Factor (C) is a term which defines the spectrum characteristics of the signal. It is a ratio between the signal peak amplitude A_{peak} and RMS value of signal power P_{RMS}. Physically, it describes how extreme the peaks are in a signal.

$$C = \frac{A_{peak}}{\sqrt{P_{RMS}}} \tag{2.3}$$

PAPR is a logarithmic indicator of crest factor for RF communication which is defined as;

$$PAPR = 20log_{10}(C^2) \tag{2.4}$$

Modulation schemes with higher crest factor tend to have higher energy content in adjacent channels causing interference. Due to systematic regulations, efficiency drops rapidly because PA is *backed-off* to operate in linear region. Table 2-1 [1] lists PAPR values for different communication standards. Over the years, as spectral efficiency or optimum bandwidth usage increases and high data rates are achieved, PAPR value has increased significantly. However PAE drops by a factor of 2 from GSM to LTE emphasizing the need to find an alternative with acceptable efficiency values for high PAPR signals.

Table 2-1: Comparison of PAPR values with PA Efficiency

Transmission Standard	Launch Year	Spectral Efficiency bits/sec/Hz	PAPR dB	PA Efficiency %
GSM	2003	0.17	0	65
W-CDMA	2003	0.1	3.4	45
HSUPA	2008	1.5	6.5	35
Wi-Fi	2008	0.9	9.0	25
LTE	2010	4.0	8.0	30

2.4 PA Basics

The RF PA is an essential device which transforms DC power into RF/microwave output power based on the input RF signal. In a communication system chain, PA sits before the radiating devices i.e. antennae as shown in the system block diagram (Fig. 2-1). In a black-box representation, output is generally a scaled version of input with the amplifier gain G being the multiplying factor (Fig. 2-2). However, in a system level analysis of PA, two very critical aspects require consideration. *'Non-linearity'* and *'Memory Effect'* of PA will be discussed in the following section.

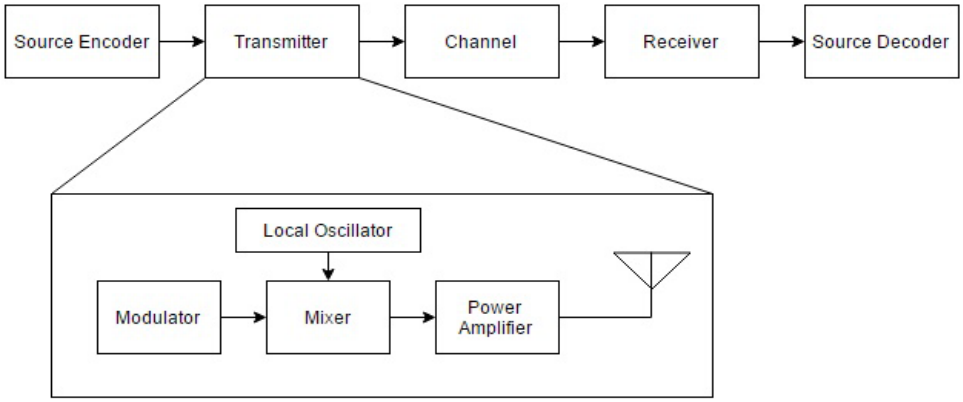

Figure 2-1: Generic Block Diagram of a Wireless Communication System

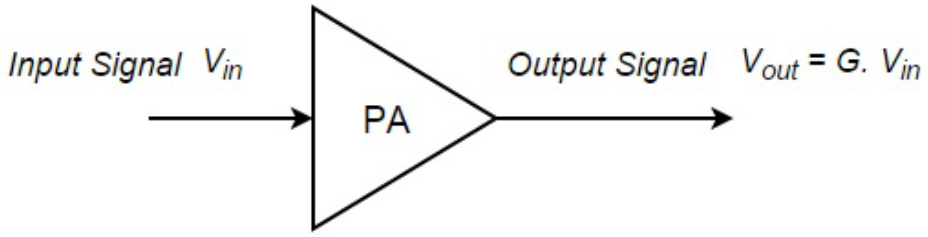

Figure 2-2: PA Block

Fig. 2-2 shows a PA block with G being the gain of amplifier. Output is however, not a linear function of input in real system as depicted by eq. 2.5.

$$V_{out}(t) = G.V_{in}(t) \tag{2.5}$$

After a certain point in the input-output curve, shown in fig. 2-3 [12], the slope drops considerably meaning that the PA is now operating in *'non-linear'* or *'saturation'* region. Increase in the input power does not reflect in the output power of the system. Traditionally, PAs are designed to draw a fixed amount of DC power. It can be seen that for real systems, the output usually curves towards the system output limit in continuous way rather than an abrupt change of gradients.

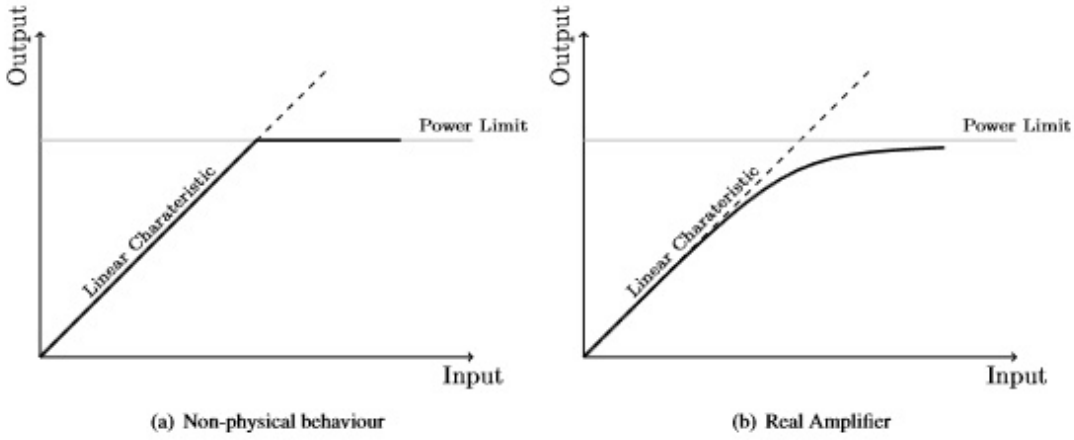

Figure 2-3: Input-Output Response curves for an Ideal and Real PA

The input-output curve is then divided into linear and compression region. It is important to note that in linear systems, the principle of superposition applies. A linear system with the model shown in equation

$$y = F\{x\} \tag{2.6}$$

will produce an output $a_1F\{x_1\} + a_2F\{x_2\}$, for an input $a_1x_1 + a_2x_2$ with a scalar multiple a, where **x** and **y** being the input and output of the system respectively. The said superposition principle does not hold true for non-linear systems and there are additional terms in frequency spectrum which are called intermodulation products or harmonics. Having established that an RF PA behaves as a non-linear system, it is now important to characterize PA behavioral model.

2.4.1 Nonlinear Memoryless Model

For narrow band signals where the envelope of input signal varies slowly, the output of PA is a function of instantaneous input value. For a limited range of input signal amplitudes, the memoryless nonlinear behavior of PA can be modeled using a complex power series [9].

$$V_{out}(t) = \sum_{k=0}^{\infty} a_k . V_{in}^k(t) \tag{2.7}$$

Where $\boldsymbol{a_k}$ is the gain of the system and it depends upon the order of the model. For the first order system, the response is linear. With the expansion of power series, the even terms (v_{in}^2, v_{in}^4, v_{in}^6 …) produce harmonics in spectrum and the odd terms (v_{in}^3, v_{in}^5, v_{in}^7, …) result in

intermodulation products. The Harmonic Distortion (HD) can be filtered out, while Intermodulation Distortion (IMD) causes a bigger concern due to that fact that it is too close to the actual signal band.

2.4.2 Memory Effect on PA Models

Memory effect in behavioral model describes the extent to which the current response of the system is influenced by past inputs to the system. It is a very critical phenomenon in PA. If the impact of memory is considered on the system model, then it cannot be represented by a simple power series expansion because the scaling factors or 'coefficients' vary for each memory tap [10, 11].

$$y[n] = \sum_{p=0}^{P-1} a^p . x[n] . |x[n]|^p \tag{2.8}$$

The equation 2.8 governs the system model for a complex memoryless behavior where a^p is the set of coefficients and P is number of coefficients of polynomial or system order. In case of memory the model takes form of the equation 2.9.

$$y[n] = \sum_{i=0}^{M-1} \sum_{p=0}^{P-1} a_{pi} . x[n-i] . |x[n-i]|^p \tag{2.9}$$

M is the number of memory taps or past terms used to calculate instantaneous output of PA and P is number of coefficients of interpolating polynomial. The delayed values of input signal are also considered in case of memory polynomial.

2.5 Performance Characterization

The accuracy and capability of PA model to mimic the real-time system can be measured using following Figures of Merit. In discrete domain, the input and output of the model is assessed sample by sample and the performance is expressed in dB for both *Normalized Mean Square Error (NMSE)* and *Adjacent Channel Error Power Ratio (ACEPR).*

$$NMSE = 10 \log \left(\frac{\sum_{n=1}^{L} |y_{real}[n] - y_{model}[n]|^2}{\sum_{n=1}^{L} |y_{real}[n]|^2} \right) \tag{2.10}$$

and

$$\mathrm{ACEPR} = 10\log\left(\frac{\int_{\mathrm{adj}}|\mathrm{Y_{real}(f)} - \mathrm{Y_{model}(f)}|^2\mathrm{df}}{\int_{\mathrm{chan}}|\mathrm{Y_{real}(f)}|^2\,\mathrm{df}}\right) \tag{2.11}$$

where y_{real} and y_{model} are the outputs of real system and the PA model respectively and *Y (f)* is the Fourier transform of output signal and power in allocated band and adjacent band is measure using the integrals.

Another important figure of merit that defines quality of the output RF spectrum which in turn translates into compliance with linearity constraints is *Adjacent Channel Leakage Ratio* (ACLR) or *Adjacent Channel Power Ratio* (ACPR). It is the ratio of power transmitted in the allocated bandwidth to the power which seeps into sidebands due to nonlinear distortion caused by PAs which are forced operated in high efficiency region.

$$ACLR = 10\log\left(\frac{\int_{f_{adj}}|Y(f)^2|df}{\int_{f_{chan}}|Y(f)^2|\,df}\right) \tag{2.12}$$

Where *Y (f)* is Fourier transform of output and $f_{adj}$and f_{chan} are bandwidth of adjacent channels and complete channel respectively. Fig. 2-4 [11] graphically depicts useful power leakage into sidebands at the output and intermodulation products.

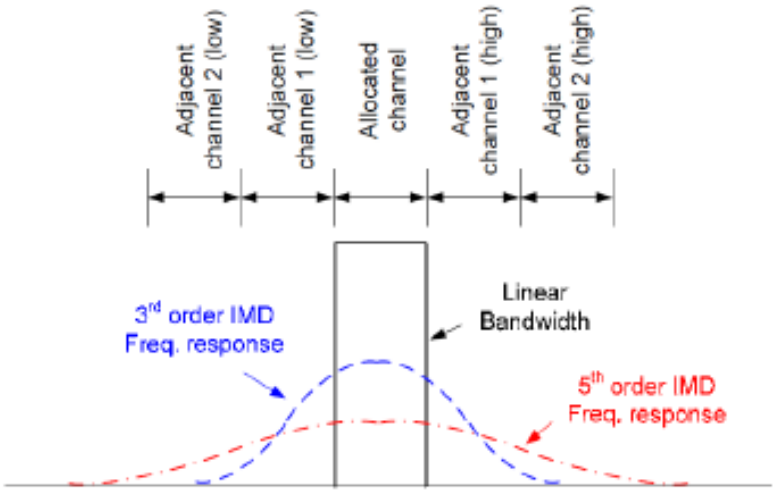

Figure 2-4: Linear Output and Intermodulation Products

2.6 PA Model Estimation

Following section provides a comparison between a memoryless PA model and one where delayed inputs also impact the output of system i.e. *'With-Memory'*. Initially a memoryless system is estimated from input and output relation of a real PA and modeled output is compared with real output to quantify the accuracy with which the *'black box'* has been modeled. Subsequently, memory is also included in the estimation and results are compared. Initial step towards PA model estimation is to get a characteristic response of PA for a predefined input test signal. Fig. 2-5 shows a simulated response of PA for a 5 MHz LTE test signal. Input signal bandwidth is 5 MHz and number of samples is 9216.

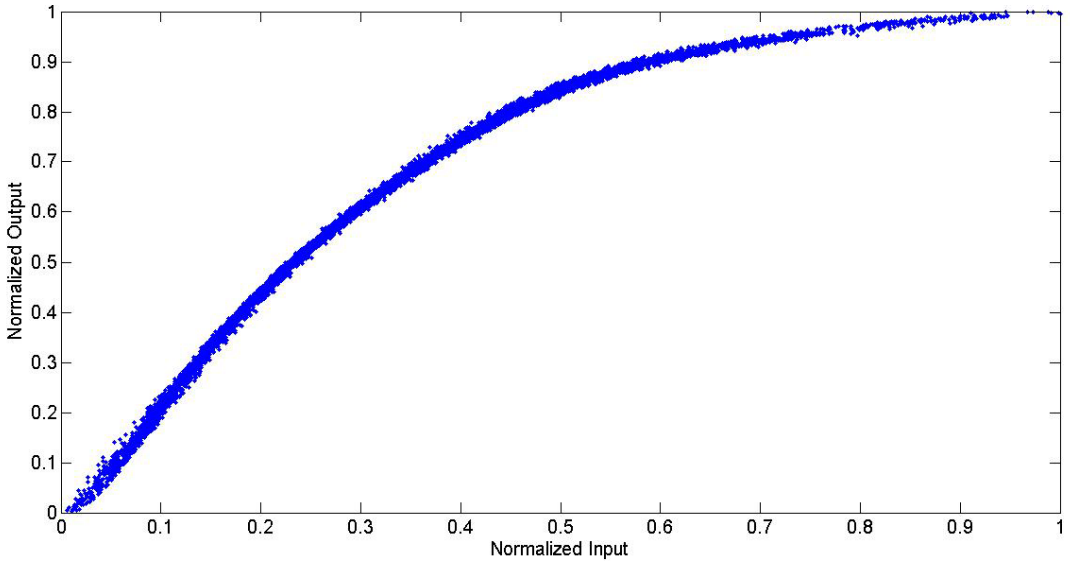

Figure 2-5: AM-AM Response of PA

A memoryless and with-memory PA model will be identified based on polynomials from eq. 2.4 and 2.5 in the following section. Fig. 2-6 and 2-7 show memoryless response and a PA model with 2 memory taps for different system order values respectively. For memoryless model identification, increasing the order of interpolating polynomial improves estimation to an extent, after which increasing the system order only adds to computational complexity with not so great effect on model quality. As we move to memory polynomial based identification of PA model with 2 memory taps, each instantaneous output is the outcome of instantaneous input and 2 previous input values. Including memory effect provides an equivalent model quality to higher order memoryless model with the use of a lower order polynomial.

Table 2-2 lists the results obtained by model estimation. Increasing polynomial order definitely produces estimation but higher order polynomial interpolation adds to computational cost which is a critical parameter for power constrained handheld devices. However, pre-calculated polynomial based model can be stored into a *Lookup Table* (LUT) which produces a fixed output value for a certain input. However, Lookup table size is defined prior to input being given to PA model. With some compromise on accuracy, the computational complexity can be reduced with a complex gain LUT. Multiple LUTs can be implemented using FPGA if memory terms are included in PA model estimation.

Table 2-2: System Order and NMSE

Polynomial Order	**Memoryless PA Model**		**PA Model with Memory (No. of Memory Taps = 2)**	
	No. of Coefficients	NMSE (dB)	No. of Coefficients	NMSE (dB)
1 (Linear)	1	-15.2191	3	-15.3867
3	3	-34.1801	9	-34.9425
5	5	-37.5177	15	-38.3528
7	7	-39.5810	21	-41.2567

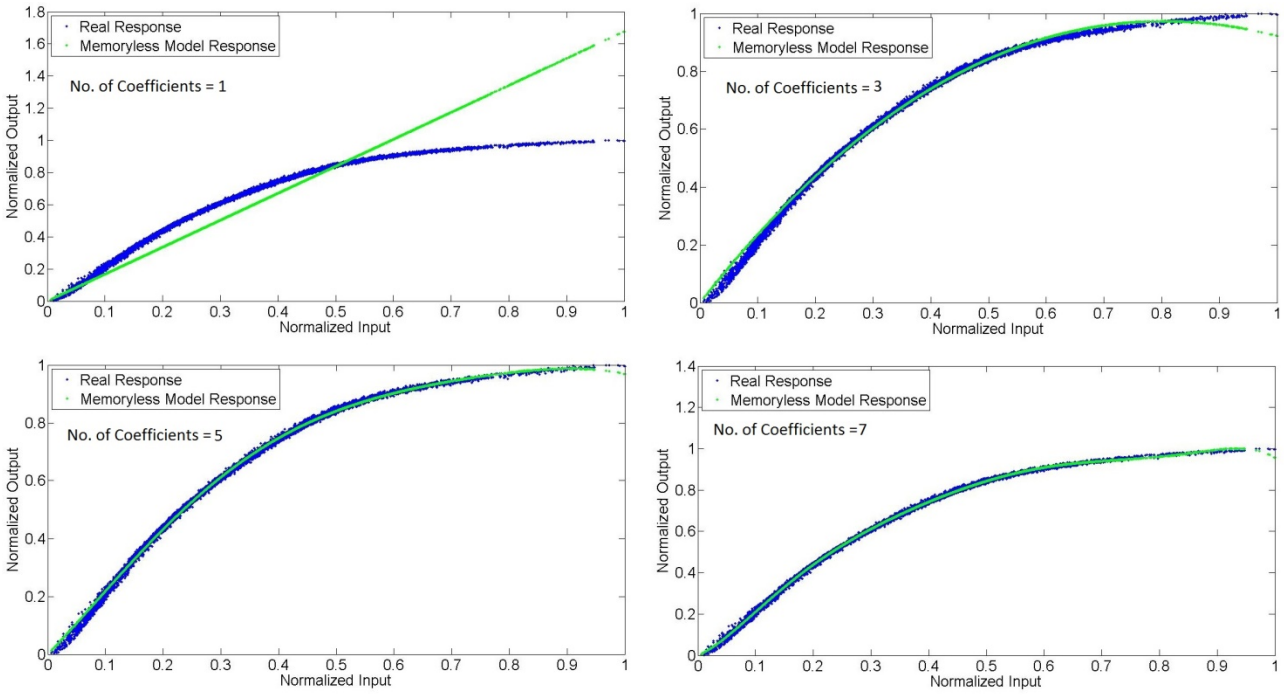

Figure 2-6: Memoryless PA Model for 5 MHz LTE Signal

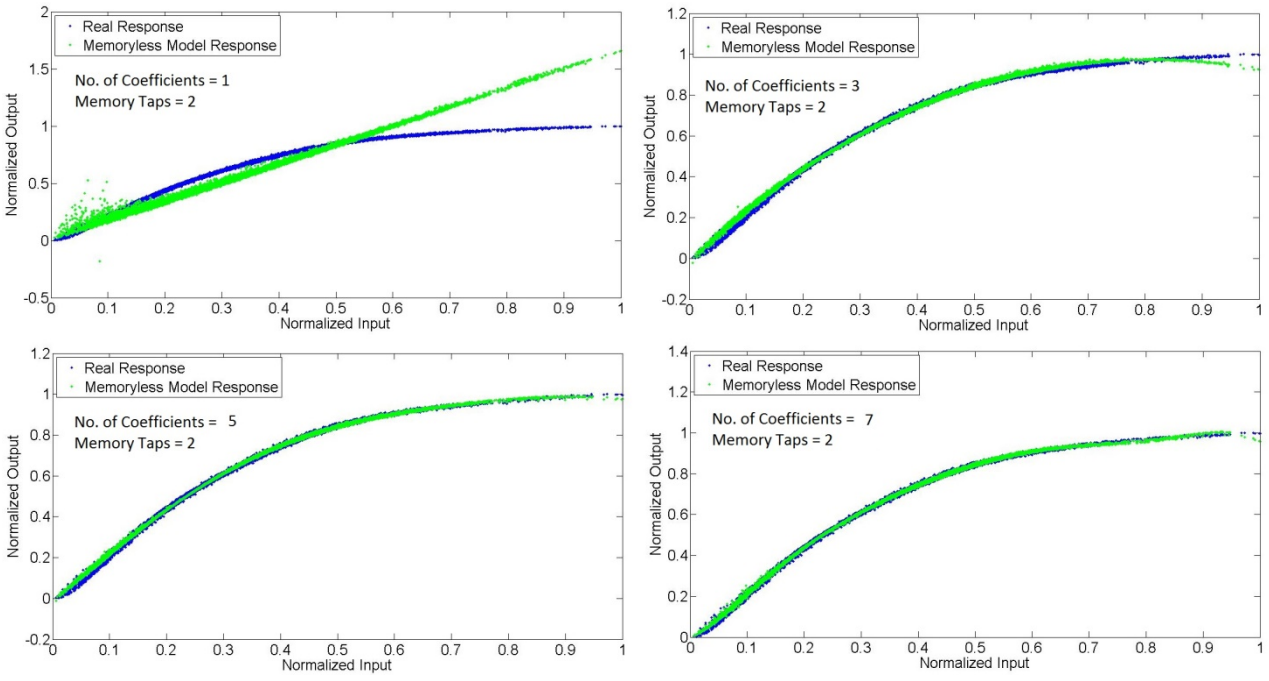

Figure 2-7: PA Model with 2 Memory Taps for 5 MHz LTE Signal

3 Envelope Tracking and Shaping for Power Amplifiers

The Envelope Tracking PA yields high efficiency when signals with high PAPR are amplified. Communication standards with spectrum efficient digital modulation schemes impose strict constraints on linearity requirements for handheld and infrastructure applications of wireless communication. An ET PA achieves considerable efficiency by modulating DC power supply instantaneously tracking a shaped envelope of input RF signal. In this chapter, basics of ET are discussed with an aim to link improved system efficiency with a dynamic supply PA technique.

3.1 Fundamentals of Envelope Tracking

The idea is to improve power efficiency of PAs with high PAPR signals. The need to achieve higher data throughput with spectrum constraints can be met with the use of complex, multicarrier modulation schemes. In a traditional fixed supply amplifier, energy is wasted when the system operates below peak output power. If the envelope of information being amplifier is constant, it is possible to adjust the supply to PA in order to optimize power utilization. The similar approach enables GSM communication to achieve efficiency as high as 65 % with the use of constant envelope signals.

However, as in LTE and other modern communication standards the signals are consistently varying and optimal solution is to dynamically modify the power supply to PA to track the requirements of signal envelope. This is achieved by performing magnitude calculation of input signal. ‘Average Power Tracking’ scheme follows a relatively slow-varying change in the output signal whereas ET updates the power supply requirement at a much faster I/Q sub-sample rate. Generalized architecture of the fixed supply, DC tracking and an ET power system is illustrated in fig. 3-1 [1].

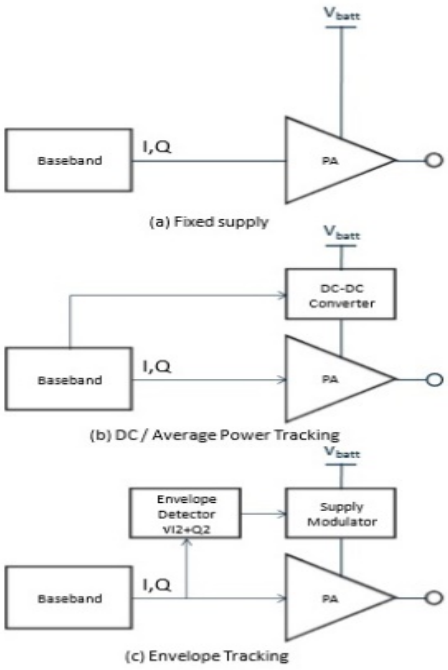

Figure 3-1: Power Supply Architecture

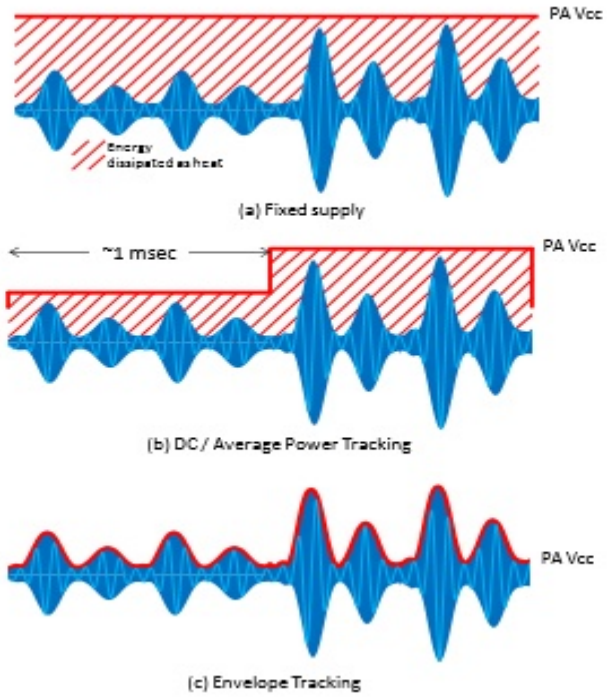

Figure 3-2: Envelope and Transmitted Power

It can be noted that envelope detection of input signal is performed in the feed-forward path and a supply modulator block varies the power to PA dynamically to enhance efficiency.

Signal's envelope for each type of supply scheme is shown in fig. 3-2 for demonstrating how the system resources are used efficiently by the tracking the RF envelope and modify the supply to PA.

As detailed in the previous chapter, a PA operates at its maximum efficiency in compression region. An obvious advantage of using ET PAs is that it can be made to operate in compression for a wider range of outputs by maintaining a lower and constantly changing power supply.

3.2 ET System Architecture

An ET PA system uses a linear or switched amplifier and a modulation circuit for supply voltage i.e. *Envelope Amplifier* (EA). In this technique, the supply voltage is dynamically varied according to magnitude calculations of input signal.

The digital data path for I/Q components which are fed to PA after mixing and filtering is similar for both fixed supply and ET PA. However in ET PA, another feed-forward path is included which tracks sub-sample level envelope. An envelope shaping function (shown in Fig. 3-3) is used to correctly identify which power supply level is suitable for incoming input signal level.

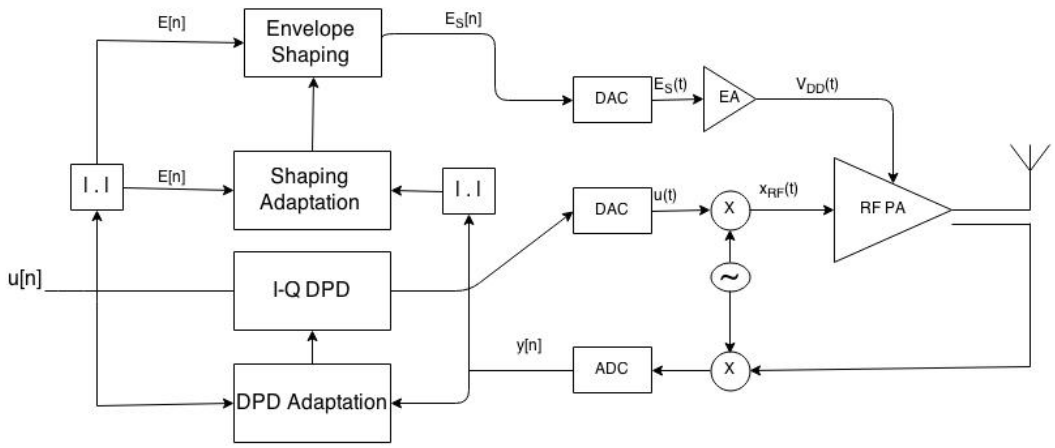

Figure 3-3: ET PA Block Diagram

From the block diagram, it can be noted that RF input signal denoted **u[n]** is fed to signal and envelope path simultaneously. In the envelope path, magnitude calculation is performed to identify the level of envelope denoted as **E[n]**. The output of envelope shaping block $\mathbf{E_s[n]}$ modulates DC power supply to RF PA. Dynamically varying power supply is beneficial but

the cost the non-linear distortion at the output. An alternative approach is to use mapping function to linearize AM-AM distortion by fixing “targeted gain” value but using an *Iso-gain Shaping* deteriorates efficiency. Additional non-linear compensation in data path is added to reduce AM-PM distortion.

3.3 Efficiency Vs Linearity for ET PAs

The concept of ET PA seems simple enough to make it an attractive alternative to fixed supply PAs for high PAPR transmission schemes, but limitations such as efficiency of PA, linearity constraints specific to each standard and output power handling capacity are weak points of schemes which employ envelope information for power supply variation.

Efficiency being the most critical figure of merit requires considerably high efficiency from power supply modulator or EA along with an RF PA which has high peak power efficiency. Whereas, low noise and linearity requirements for ET technique mean that not only RF PA distortion should be controlled but also the distortion from supply modulating amplifier should be kept on a minimum. Consequently, a tradeoff between PA efficiency and compliance with linearity restriction is not only dependent on amplifier design but also on supply modulator design and baseband processing.

Another important challenge in small terminal PA design and operation is handling of bandwidth and the ability of PA to operate over various frequency bands. W-CDMA devices may have to support to support operation across five bands because of world-wide coverage and there lies the need for three separate sets of PA assembly [1]. This trend is going to demand the operation across wider bands from future devices. There are various techniques to improve efficiency when an RF PA is deployed with a supply modulator.

3.4 Performance Enhancement of RF PA

Generally, operating a PA in compression maximizes its efficiency and this is evident from the performance of constant envelope modulation schemes e.g. GMSK used in GSM which do not include *Amplitude Modulation* (AM) component. But for a modulation scheme that includes an AM component, the output of the system will show AM-AM distortion or ‘clipping’ if the input signal has higher instantaneous PAPR and drives PA to operate in compression. For such schemes, the PA is made to operate below the maximum output levels so that instantaneous input envelope level itself does not cause output distortion.

One of the performance limiting factors for ET PAs is spectral regrowth. As discussed in previous sections that in compression PA output AM-AM and AM-PM response is distorted due to non-linearity. Therefore, frequency spectrum shows a stepped down degradation energy content of the signal in adjacent channels. Each step represents the amount of useful power being leaked to sidebands. This phenomenon is known as spectral regrowth. In order to compensate for the said distortion, a powerful linearization technique is needed.

3.4.1 Digital Pre-Distortion

Pre-Distortion is a technique that significantly reduces AM-AM distortion by applying an 'inverse' distortion to signal. Once the signal is compressed by PA, the inverse distortion is cancelled out by PA's AM-AM distortion property and a fairly correct signal is produced at the output of RF chain. The amount of distortion needed to rectify PA's nonlinear impact is estimated using a feedback path. Fig 3-4 [7] depicts the general idea of DPD process.

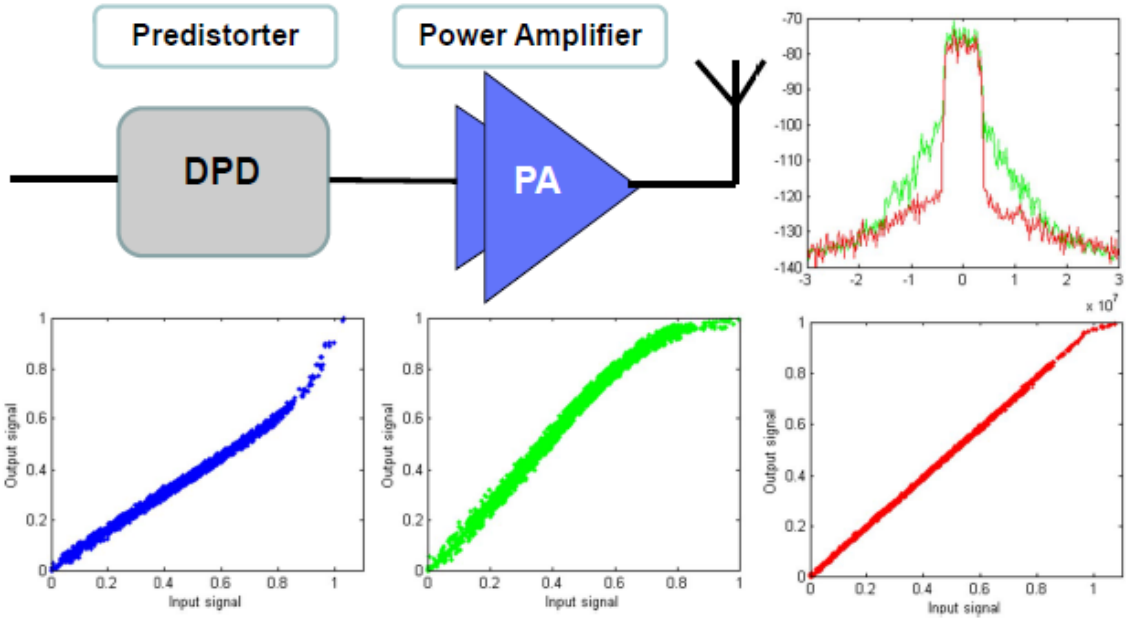

Figure 3-4: DPD Principle with Resultant Signal Spectrum

PA response is prior to applying an input to the system using test signal. An inverse of PA characterization is applied to input signal and the result presents a fairly linear signal at PA output. Frequency spectrum in Fig. 3-4 [7] shows improvement in terms of power leakage into sidebands. This enables the possibility to use a PA at maximum output level, enhancing the efficiency of a standard amplifier assembly. Since it a computationally complex and a

significant amount of signal processing is applied to baseband signal before it is input the PA, this technique is not too feasible to be used for power-constrained, non-infrastructure small communication modules.

DC-Tracking or Average Power Tracking is another solution which benefits from the fact that base stations and small terminals do not always transmit at their maximum power. Protocols “hand-shake” for the requires output power levels for a given time and power supply to PA or *Drain Supply* can be adjusted to lower values which in turn improves power efficiency to some extent.

This leads to ET PA which keeps tracks of instantaneous level of input signal, and adjusts the power supply to match RF signal at the input of PA. Fig. 3-5 [1] shows device efficiency versus output power for over a range of supply voltages.

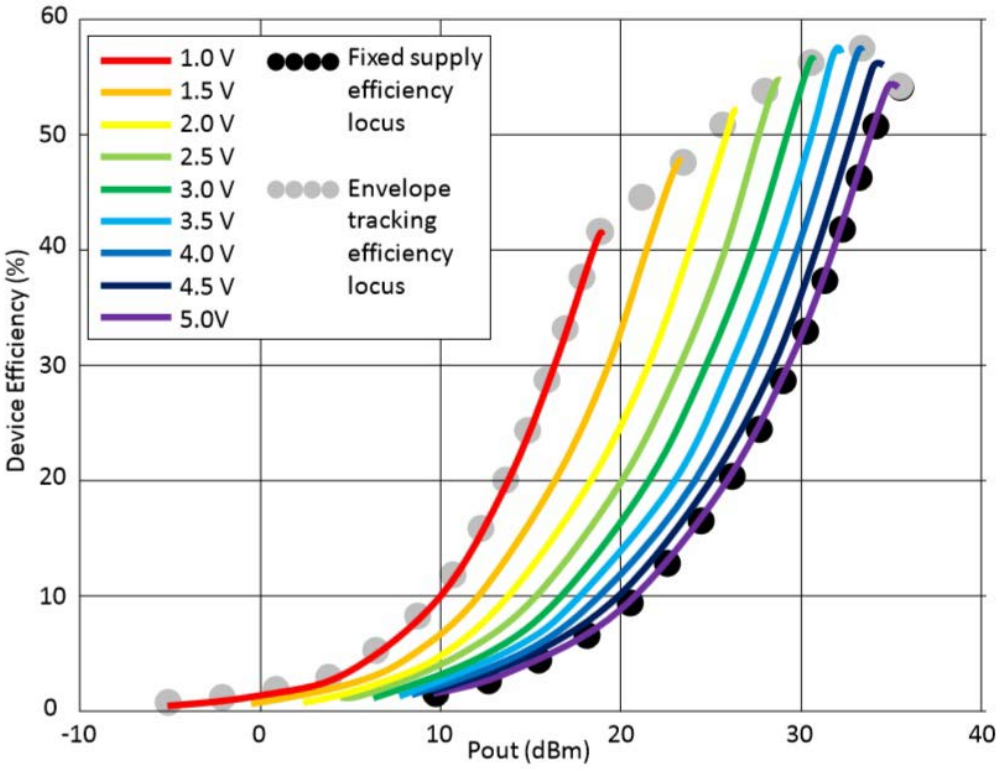

Figure 3-5: Device Efficiency and Output Power

It can be seen that in case of a fixed supply PA, efficiency drops significantly when the system is operated below maximum output power. However, dynamic supply with envelope shaping function offers relatively constant efficiency even at lower values of output power.

3.5 Envelope Shaping Function

The shaping function is responsible for performance improvement of system. A DAC and filter converts the output of shaping block into a nominal envelope waveform which is fed to supply modulator or EA. It is however, very critical to understand the concept of path synchronization. 'Signal Path' and 'Envelope Path' must be aligned in timing and magnitude so that correct sample of information is amplified with correct level of supply. Following objectives can be achieved using shaping by means of changing power supply requirement;

- Optimum Efficiency Shaping
- Iso-Gain Shaping

Optimum Efficiency Shaping function results in relatively constant system efficiency across a range of output power. PA is operated at maximum efficiency for different supply voltages. This technique however, introduces AM-AM distortion in the output. Gain characteristics and Optimum efficiency curves are shown in fig. 3-6 [9].

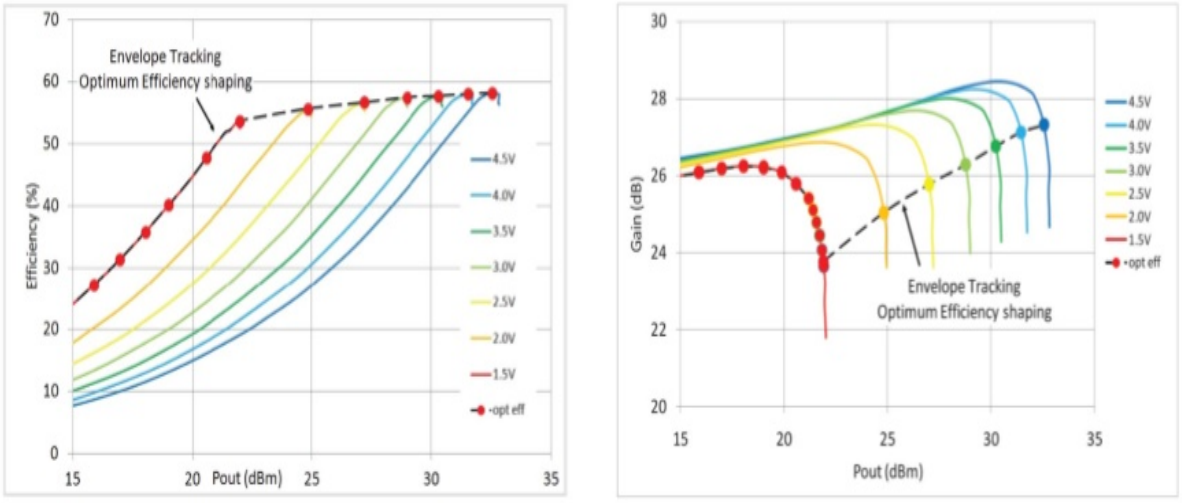

Figure 3-6: Efficiency and Gain Vs System Output (Optimum Efficiency Shaping)

Iso-Gain Shaping optimizes the system to achieve a lower AM-AM distortion by fixing a value for targeted output gain although the system operates in compression. In other words, linearity is achieved while sacrificing efficiency. Iso-gain shaping provides greater degree of compression for highest power levels resulting in absolute energy savings.

3.5.1 Adaptive Iso-Gain Shaping Model

The advantage to use an adaptive iso-gain shaping function it is to avoid generating prior input-output characterization of PA using different supply voltages. Fig. 3-7 shows block diagram of an ET PA which uses an adaptive envelope tracking and shaping function as well as Digital Pre-Distorter (non-linear modulation) to compensate for AM-PM to some extent. A mathematical model is developed in this section which represents the behavioral model of an adaptive shaping block.

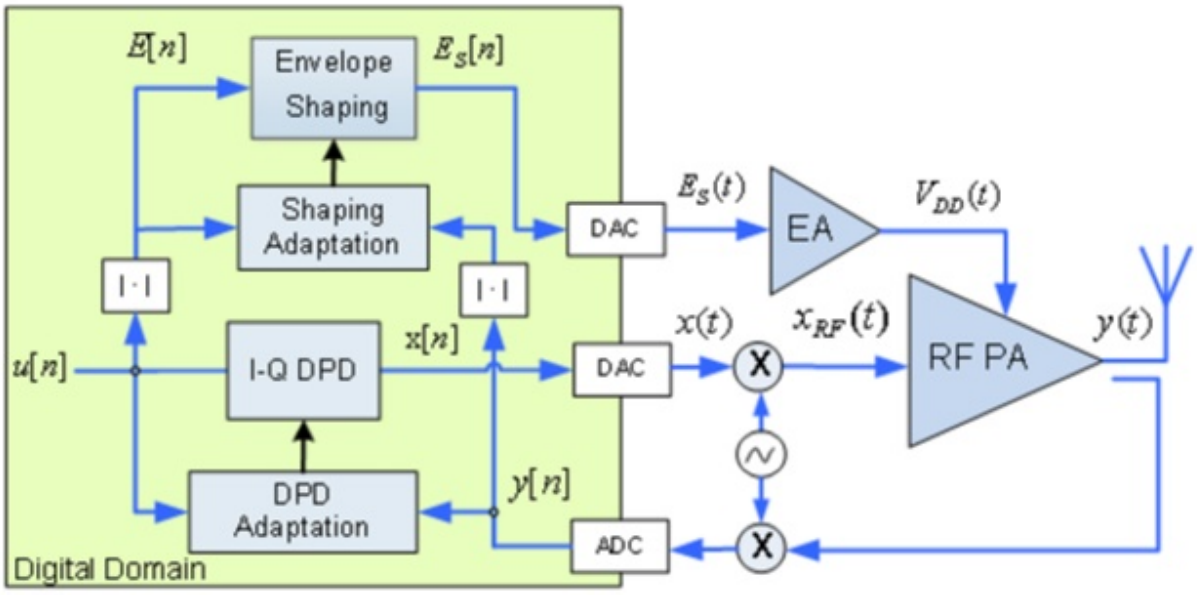

Figure 3-7: ET PA with Envelope Shaping Block

Working in discrete domain, the complex baseband is designated as ***x[n]***. The first step is to perform magnitude calculation for envelope;

$$E[n] = |x[n]| = |\, x_I[n]^2 + x_Q[n]^2| = \sqrt{x_I[n]^2 + \, x_Q[n]^2} \tag{3.1}$$

The output of model $E_s\,[n]$ considering memory terms can be written as;

$$E_s[n] = \sum_{i=0}^{N-1} \sum_{p=0}^{P-1} w_{p,i}.\,(E[n-\tau_i])^p \tag{3.2}$$

τ_i is the most significant delay of the envelope that can be used to incorporate memory. The output of the shaping model $E_s\,[n]$ can be written as the difference of signal envelope and a non-linear distortion estimated using system coefficients.

$$E_s[n] = E[n] - \varepsilon[n] \tag{3.3}$$

and

$$\varepsilon[n] = \mathbf{E_n}.\mathbf{w_n} \tag{3.4}$$

$\mathbf{w_n}$ is a vector of coefficients of order **'O'** where O = P×N. P is the system order or the no. of polynomial coefficients and N is the no. of memory taps. Data matrix for calculation of system coefficients consists of vectors of basis waveform and represented as $\Phi = (\varphi_1, \varphi_2, \ldots, \varphi_L)^T$, where L is the no. of data samples. Any vector of the data matrix can be written as $\varphi_n = (E[n], E[n]^2, \ldots, (E[n])^p, \ldots, E[n-\boldsymbol{\tau}_{N-1}], \ldots, (E[n-\boldsymbol{\tau}_{N-1}])^p$

In order to make the algorithm adaptive, close loop identification approach is considered here which updates the system coefficients based on LS algorithm.

$$\mathbf{w_{n+1}} = \mathbf{w_n} + \boldsymbol{\mu}\,(\boldsymbol{\Phi}^{\mathbf{H}}\,\boldsymbol{\Phi})^{-1}\boldsymbol{\Phi}^{\mathbf{H}}\mathbf{e} \tag{3.5}$$

e is an error vector of length L and μ is the weighting factor.

$$\mathbf{e} = \left|\frac{\mathbf{y}}{\mathbf{G_0}}\right| - \mathbf{E} \tag{3.6}$$

$\mathbf{G_0}$ is the linear gain of PA in order to target a particular isogain shaping whereas **y** and **E** are PA output and signal envelope vectors, respectively.

In order to reduce the computational complexity, the isogain shaping polynomial interpolation and estimation can be replaced by Look-Up table. Equation 3.7 presents LUT model with G_{LUT} being the complex gain for each memory tap.

$$E_s[n] = \sum_{i=0}^{N-1} E[n-\tau_i].G_{LUT_i}(E[n-\tau_i]) \tag{3.7}$$

3.6 Manual Envelope Shaping and Spline Model

Shaping function uses polynomial interpolation for estimating the response of PA. However, in data estimation and statistical analysis, spline Interpolation technique is preferred over polynomial interpolation because the estimation error can be reduced even when the system order is relatively lower. This reduction in model estimation error gives rise to improved efficiency. Spline interpolation provides stability between N+1 data points by avoiding wild oscillations while forcing the first and second derivatives to be continuous.

Originally, the word ‘spline’ was used for elastic rulers that were bent in order to pass through various points called ‘knots’. The first and last or boundary points in a data set are called ‘exterior knots’ whereas all other points are called ‘interior knots’. This technique was used to make technical drawings in shipbuilding. An example of a typical spline is shown in fig. 3-8. It can be noted that the gradient of function is continuous and presents stability while fitting is performed between data points.

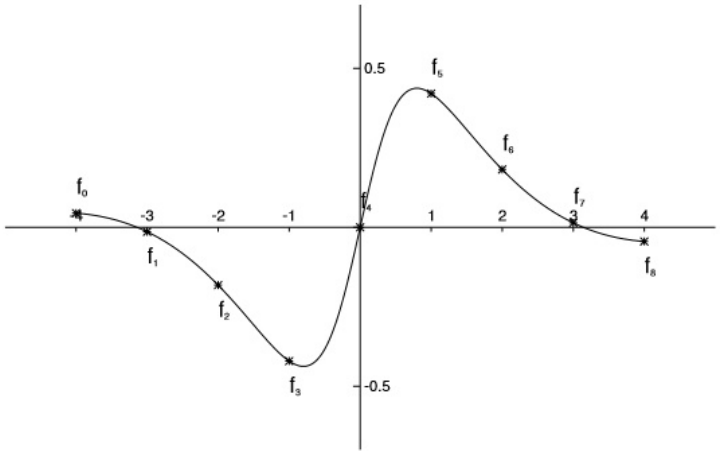

Figure 3-8: Spline Fitting

The importance of stability and continuous higher order derivatives is very significant in physical phenomenon like displacement, velocity and acceleration of moving objects and trajectory estimation functions because it minimizes potential energy of function relative to interpolation constraints. Spline interpolation scheme’s stability increases with the increase in the order of the function itself. Linear or Piece-wise continuous spline is the first order spline function, whereas quadratic and cubic spline functions are higher dimensions of spline interpolation with cubic splines being the most preferred since these offer a continuous first and second derivate.

3.6.1 Linear Splines

Linear or 1st order spline interpolation simply joins two consecutive data points using a straight-line (linear equation). It does not include any information about the impact the rest of data points can have on the fitting.

A set of *n+1* data points $((x_0, y_0),\ (x_1, y_1),\ (x_2, y_2), \dots ,\ (x_n, y_n))$ can be fit on linear splines with following function. $y_i = f(x_i)$.

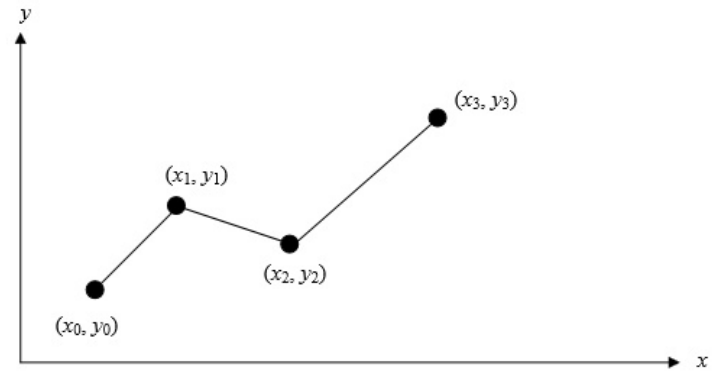

Figure 3-9: Linear Splines

For each interval ($x_i \leq x \leq x_{i+1}$), an independent linear equation is calculated which is only impacted by boundary knots.

$$f(x) = f(x_i) + \frac{f(x_{i+1}) - f(x_i)}{x_{i+1} - x_i}(x - x_i) \qquad x_i \leq x \leq x_{i+1} \tag{3.8}$$

It can be noted that $\frac{f(x_{i+1})-f(x_i)}{x_{i+1}-x_i}$ is local slope for every interval. In order to understand the concept of spline interpolation $y = \sin(x)$ is taken as an example function. Fig.3-10 shows the linear spline model output in comparison with actual values of sine function.

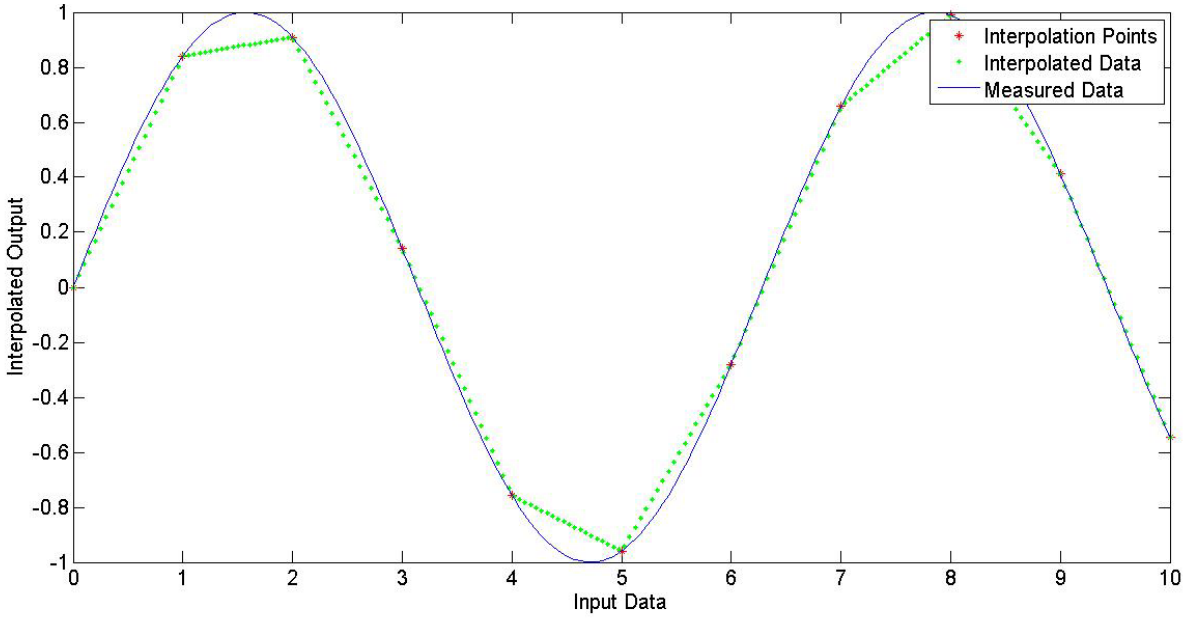

Figure 3-10: Linear Spline Interpolated Sine function

3.6.2 Quadratic Splines

In quadratic splines, each set of points is connected using a quadratic equation. This model provides estimation with less steeper change of direction at the interior knots. A given set of data points $((x_0, y_0),\ (x_1, y_1),\ (x_2, y_2), \dots ,\ (x_n, y_n))$ fits through interior knots using following algorithm;

$$f(x) = a_1x^2 + b_1x + c_1, \qquad x_0 \le x \le x_1$$

$$= a_2x^2 + b_2x + c_2, \qquad x_1 \le x \le x_2$$

.

.

.

$$= a_nx^2 + b_nx + c_n, \qquad x_{n-1} \le x \le x_n$$

In order to solve this system simultaneously, 3n equations are required to calculate 3n coefficients. Following conditions characterize quadratic splines;

Each quadratic spline passes through 02 consecutive data points.

$$a_ix_{i-1}^2 + b_ix_{i-1} + c_i = f(x_{i-1}) \tag{3.9}$$

$$a_ix_i^2 + b_ix_i + c_i = f(x_i) \tag{3.10}$$

$i = 0,1,2, \dots, n$. Since there are *n* splines passing through *n-1* interior knots. This condition yields 2n equations.

The first derivative of consecutive splines is continuous at the interior knots.

For instance, the first derivative of first spline is: $2a_1x + b_1$

First derivative of second spline is: $2a_2x + b_2$

Making derivatives equal at interior knot $(x = x_1)$ gives: $2a_1x_1 + b_1 - 2a_2x_1 - b_2 = 0$. Generalizing the expression for all interior knots;

$$2a_ix_i + b_i - 2a_{i+1}x_i - b_{i+1} = 0 \tag{3.11}$$

The above condition provides *n-1* equations. 1 remaining equation is obtained by assuming that the ***first spline is linear.*** Solving the system of equations in matrix form, results in a vector of coefficients which are then used to estimates data between known points. It is extremely important to note that for each interval, a separate set of coefficients for quadratic equation is used for a precise model.

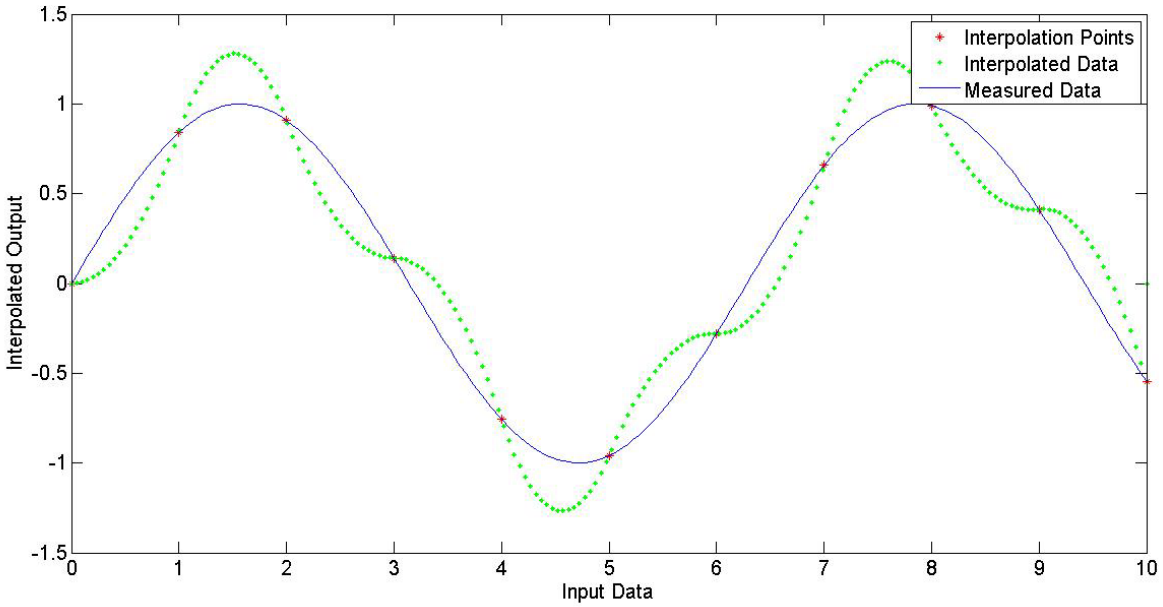

Figure 3-11: Quadratic Spline Interpolated Sine function

As shown in fig. 3-11, the interpolated function is always continuous at the interior knots i.e. there are no sharp changes in the direction which is a prominent characteristic of spline interpolation. However the data fitting is not as accurate as required to justify the selection of model. Therefore, cubic splines are preferred due to the fact that they provide more stability and accuracy.

3.6.3 Cubic Splines

Cubic spline interpolation uses a continuous first and second derivative at the interior knots. This along with the use of boundary conditions provides more stability and a smooth estimation of model. Therefore, cubic spline interpolation can replace polynomial interpolation for shaping function block used in envelope path. General form of a cubic spline interpolation model is;

$$f_i(x) = a_i x^3 + b_i x^2 + c_i x + d_i \qquad i = 1,2,\dots,n \;\; and \; x_{i-1} \leq x \leq x_i \qquad (3.12)$$

In order to solve s system of n cubic splines, 4n equations are needed to determine 4n coefficients. For a given set of data points $((x_0, y_0),\ (x_1, y_1),\ (x_2, y_2), \dots ,\ (x_n, y_n))$, following set of conditions governs cubic spline algorithm;

Each cubic spline passes through on end of the particular interval.

$$a_i x_{i-1}^3 + \ b_i x_{i-1}^2 + c_i x_{i-1} + \ d_{i-1} = f(x_{i-1}) \tag{3.13}$$

$$a_i x_i^3 + \ b_i x_i^2 + c_i x_i + \ d_i = f(x_i) \tag{3.14}$$

The above condition provides 2n equations for system.

Consecutive splines have continuous first derivative at interior knots.

n-1 equations are obtained from mathematical interpretation of the condition above similar to quadratic splines.

$$3a_{i-1} x_{i-1}^2 + 2b_{i-1} x_{i-1} + \ c_{i-1} - \ 3a_i x_{i-1}^2 - 2b_i x_{i-1} - \ c_i = 0 \tag{3.15}$$

Consecutive splines have continuous second derivative at interior knots.

The above condition provides another set of n-1 equations.

$$6a_{i-1} x_{i-1} + 2b_{i-1} - \ 6a_i x_{i-1} - 2b_i \ = 0 \tag{3.16}$$

Second derivative of first and last spline at starting and ending exterior knot, respective is equal to zero (Natural Boundary Condition).

Natural boundary conditions provide 2 equations as follows;

$$6a_1 x_0 + 2\ b_1 = 0 \tag{3.17}$$

$$6a_n x_n + 2\ b_n = 0 \tag{3.18}$$

In matrix notation, the coefficient vector **x** will have 4n elements. Solving a system of matrices will result in a cubic spline based model.

$$\mathbf{Ax} = \mathbf{b} \tag{3.19}$$

The solution for coefficients resembles the polynomial model described in previous section. Using equations 3.13 to 3.18, a data matrix **A** is constructed using input signal values. PA output response replaces vector **b** and matrix multiplication yields **x** vector. 4n elements in **x** state that each cubic spline has independent set of 4 coefficients which are used whenever an input sample value falls in the interval interpolated by the particular spline equation.

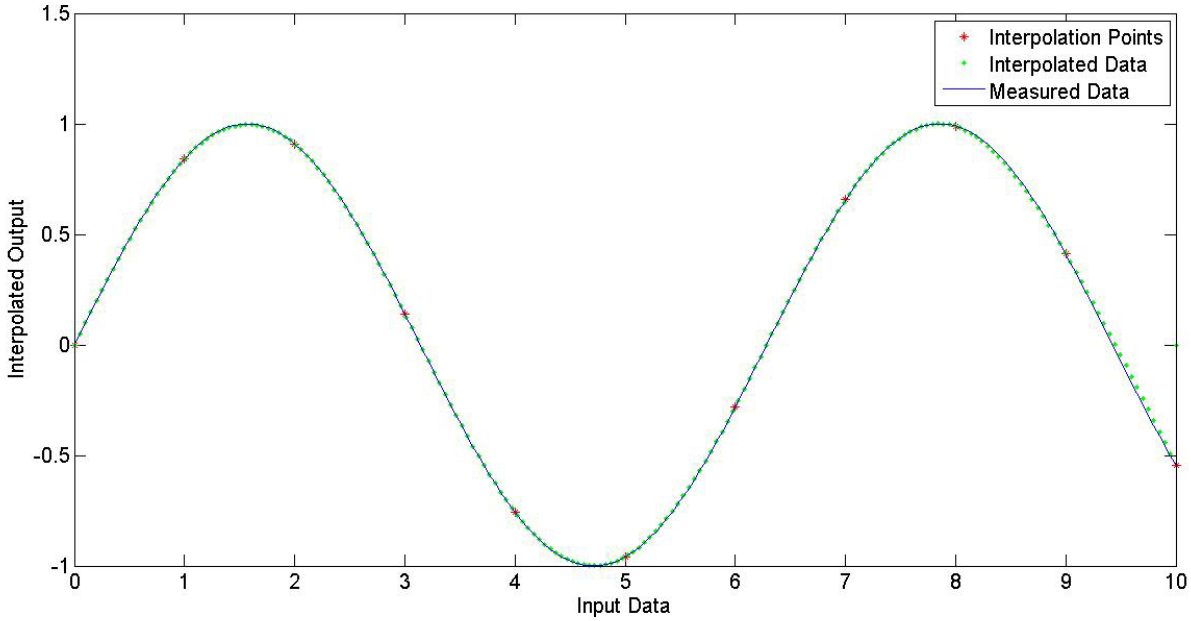

Figure 3-12: Cubic Spline Interpolated Sine function

Table 3-1: Spline Model Estimation performance for sinusoidal test function

Order of Spline	NMSE [dB]
Linear	-21.0261
Quadratic	-10.6409
Cubic	-24.9321

Table 3-1 lists NMSE values for three different types of spline interpolation (presented in section 3.6.) with a sinusoidal test function $y = \sin(x)$ to comprehensively visualize the stability property of spline interpolation. Because the number of interpolation points (11) is sufficient for the size of test vector (200 equi-spaced points), there is not a significant difference in quality of linear and cubic splines. However, the stability characteristics (shown in fig. 3-12) and close to real estimation by cubic spline makes it an alternative to replace polynomial interpolation in envelope shaping block for model estimation. Cubic spline

interpolation model will be presented as an alternative to polynomial model for manual shaping block.

3.7 Manual Isogain Shaping

Following section discusses the prospect of using manual envelope shaping (by hand) using cubic spline interpolation model established in 3.6.3 instead of using polynomial interpolation. It has been discussed how using spline interpolation improves stability of estimated data. The input-output response or the transfer function of PA is characterized using a 5 MHz LTE signal. PA is supplied with a set of drain voltage based on input signal envelope and response in terms of input power, output power and gain has been plotted. Fig. 3-13 shows voltage supply level and a back-off factor plot. Starting from a maximum drain supply voltage 28 V, PA output power response is characterized for same test signal. The supply voltage drops with a back-off factor while the lower power input samples are in line to be transmitted. It is important to correlate color coding of back-off value to gain vs output power curve presented in fig. 3-14.

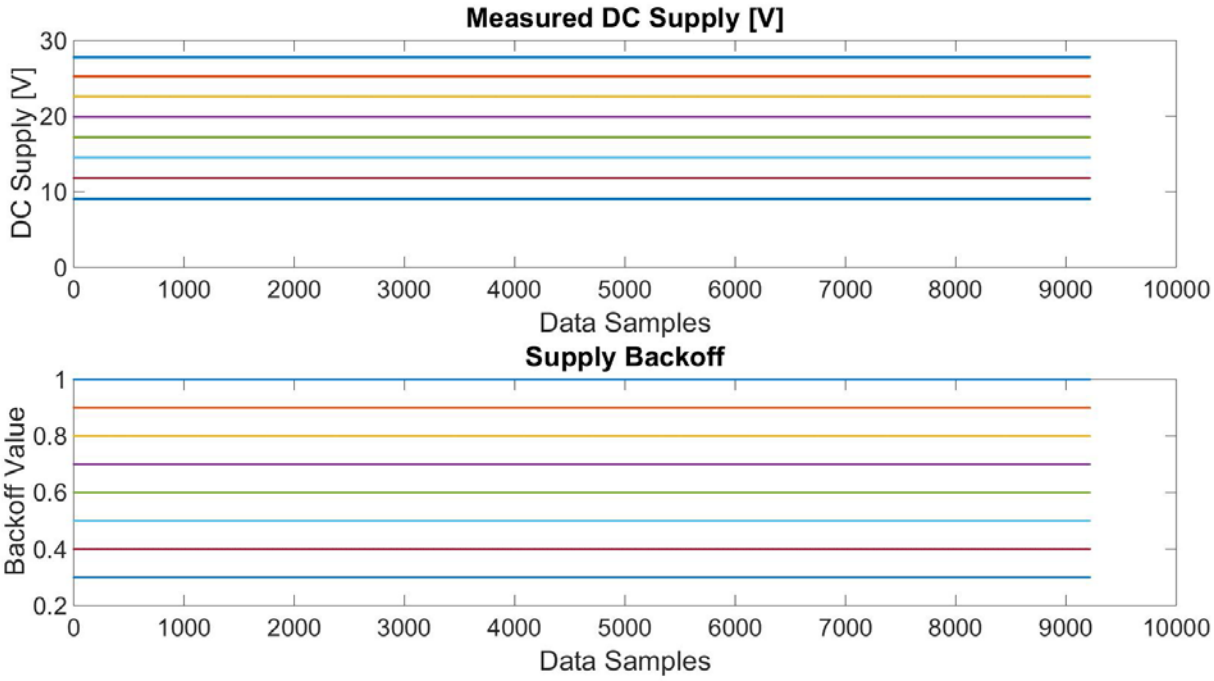

Figure 3-13: Measured DC Supply and Back-off for LTE 5MHz signal

In this simulation, the controllable parameter is *'targeted gain'*. The compromise however is between efficiency and gain.

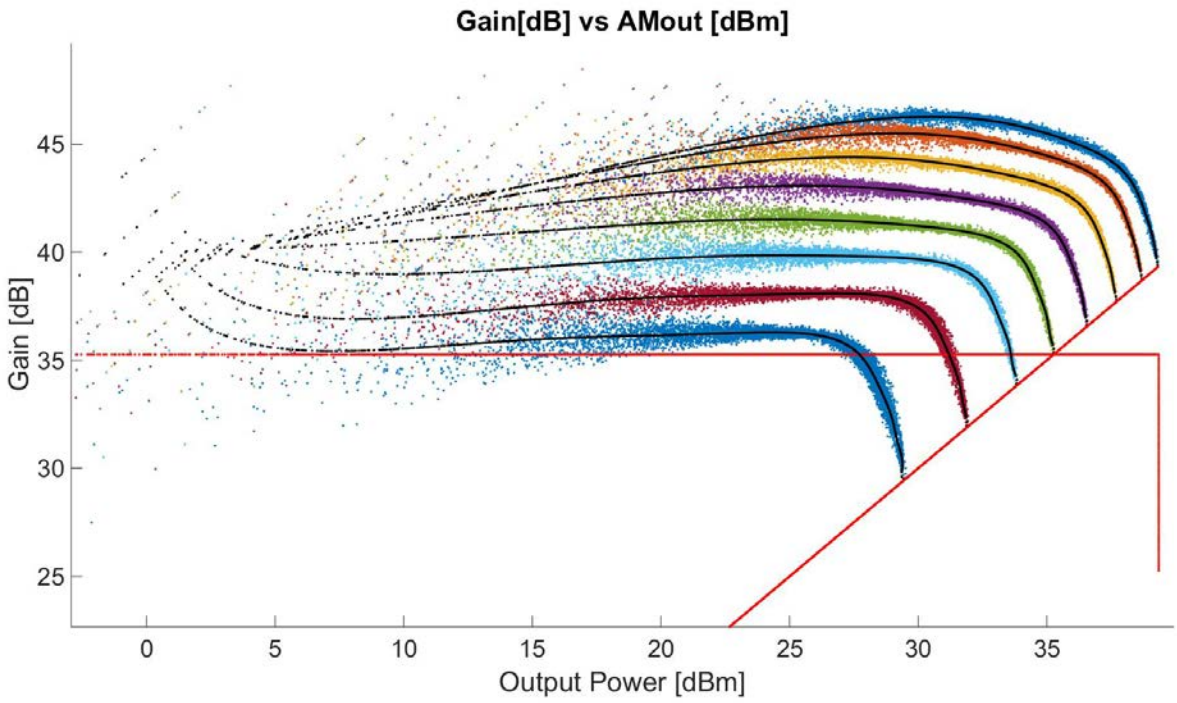

Figure 3-14: Gain vs Output Power for LTE 5MHz signal

As shown in fig. 3-14, lower power supply curves mean the efficiency increases but with that gain drops. Alternatively, when higher gain is targeted at the output, there is a greater chance of system using more resources than required which impacts adversely on efficiency. For example, an output power of 35.267 dBm is achieved here using a 17.22V power supply with a gain of 35.267 dB. Similar output power can be achieved using 19.89V, 22.57V power supply with an improved gain value of around 41dB and 43dB respectively.

3.7.1 Isogain Line or Targeted Gain

By fixing the output targeted gain, it is convenient to estimate system response by making PA operate in compression region most of the time. Fig. 3-15 shows input power vs gain of PA for a targeted gain of 35.2667dB. Input values with dBm units are translated to input signal's envelope by equation 3.20.

$$Input\ Power\ [dBm] = 20log_{10}|\text{xBB}| \tag{3.20}$$

|xBB| is the instantaneous value of input signal envelope. Fig. 3-16 shows the similar set of power supply curves for a targeted gain value of 39.267dB.

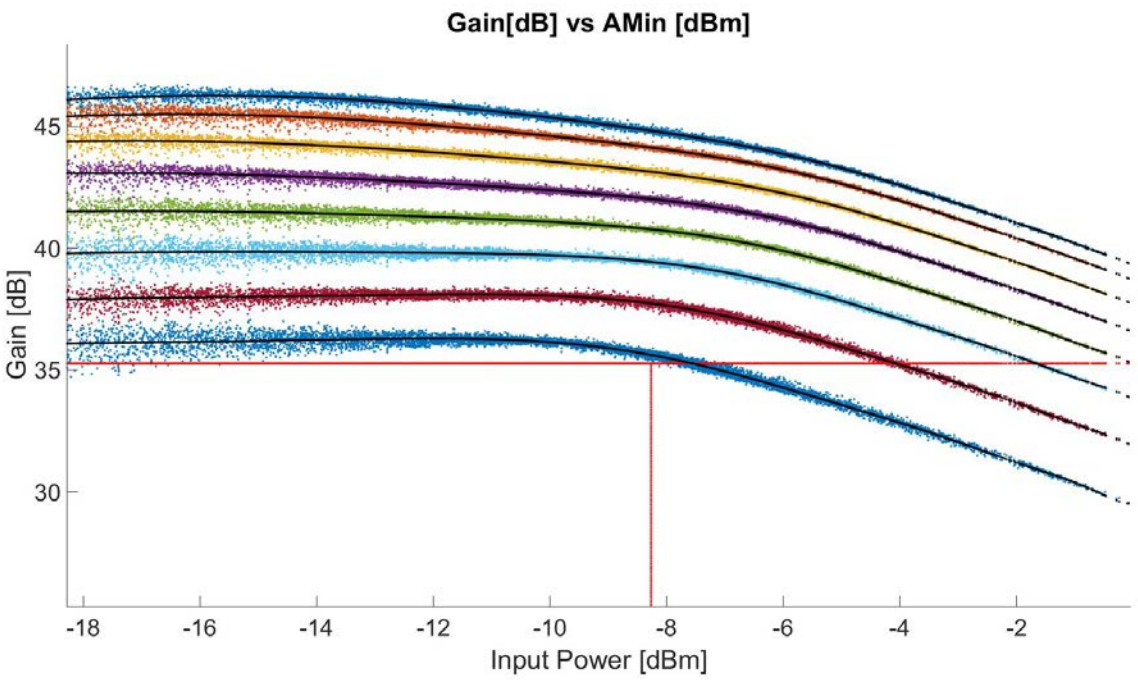

Figure 3-15: Gain vs Input Power (Targeted Gain = 35.2667dB)

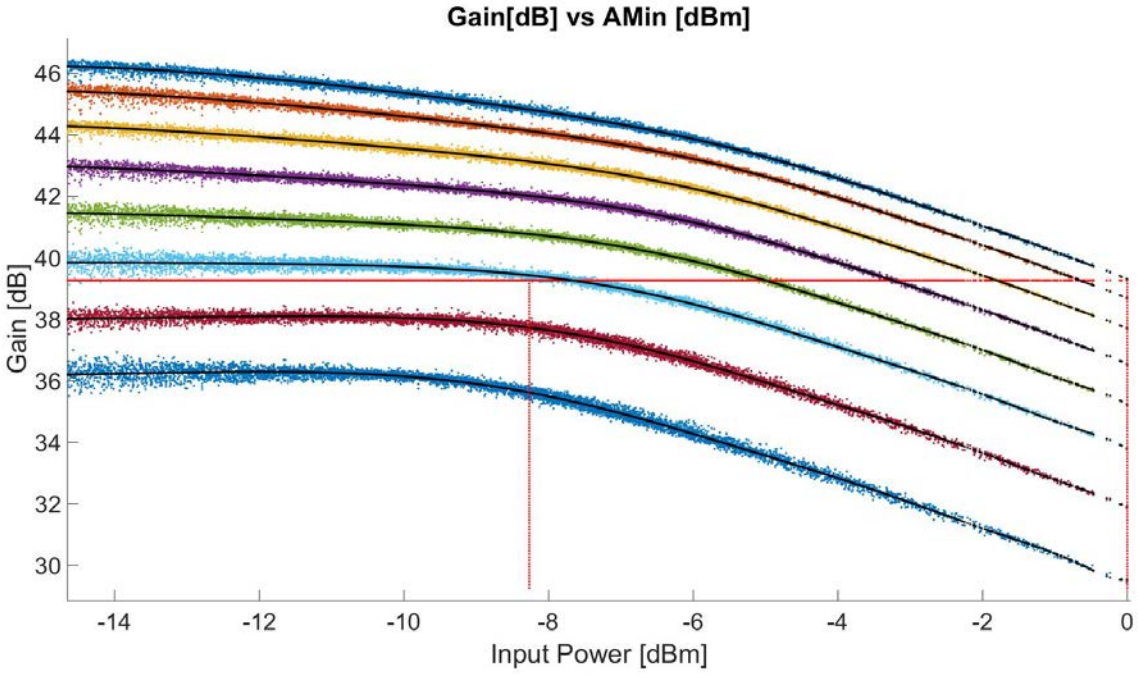

Figure 3-16: Gain vs Input Power (Targeted Gain = 39.267dB)

4 Experimental Setup

This chapter starts with the introduction to hardware setup which has been used to validate the adaptive envelope shaping algorithm. MATLAB simulation for Manual Isogain Shaping with a cubic spline interpolation model is preceded by the DUT results which show system performance for adaptive ET and shaping as well as with an IQ DPD. Test results show that the inclusion of an I-Q DPD in the signal path can improve performance to a certain extent while combating AM-PM distortion.

System-level testing and validation provides a better measure of performance for an algorithm as compared to MATLAB based simulations because of the fact that PA behavioral model cannot be accurately estimated over all the dynamic operational range. Therefore, an out-of-range response might cause adaptive shaping process to diverge.

4.1 Device-Under-Test Setup

The functional block diagram of hardware setup used to test the algorithm is displayed in the fig. 4-1. After performing the digital signal processing via MATLAB, the signal is sent to PA using DAC board. The PA used in the testbed is a broadband high efficiency continuous-mode class-J amplifier with center frequency at 950MHz based on CGH35030F packaged GaN HMET from Cree Inc.

Once the signal is processed and converted from digital to analog domain, it is then modulated using a 950MHz carrier provided to Texas Instruments pattern generator board by Agilent MXG N5182A local oscillator. Modulated signal vector is given to Tabor Electronics PM8572 waveform generator. The output is fed into Agilent DSO9404A oscilloscope to observe shape of modulated signal wave. Output from waveform generator is given to supply modulation circuit implemented on LT12100 integrated circuit which dynamically varies DC power supply voltage coming from R& S HMP4040. The modulated or up-converted signal is fed to an EA which modifies the supply circuitry to PA based on the envelope of the input signal. After the output of RF PA stage is attenuated, the signal is fed back to PC for performance analysis while DSO9404A oscilloscope captures the output data to compare input and output waveforms. Frequency spectrum of RF output signal is displayed at Agilent Tech. MXA N9020A signal analyzer. Fig. 4-2 shows the layout of instruments at testbed.

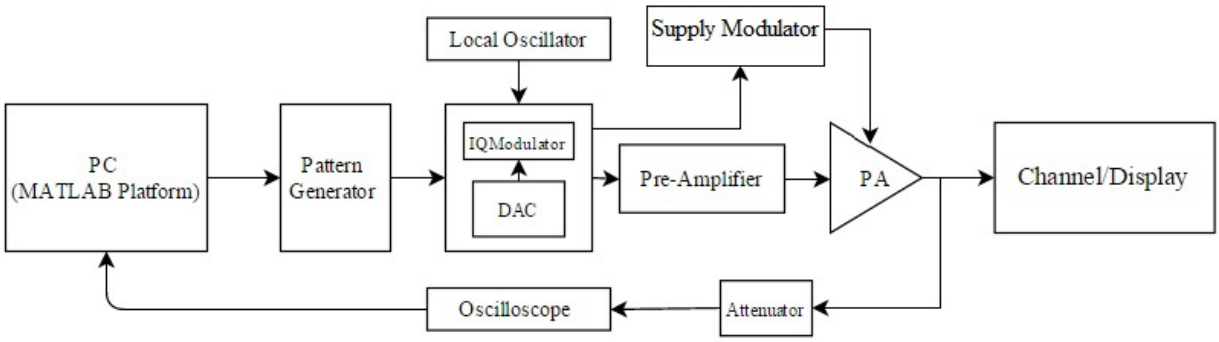

Figure 4-1: Block Diagram of Testbed

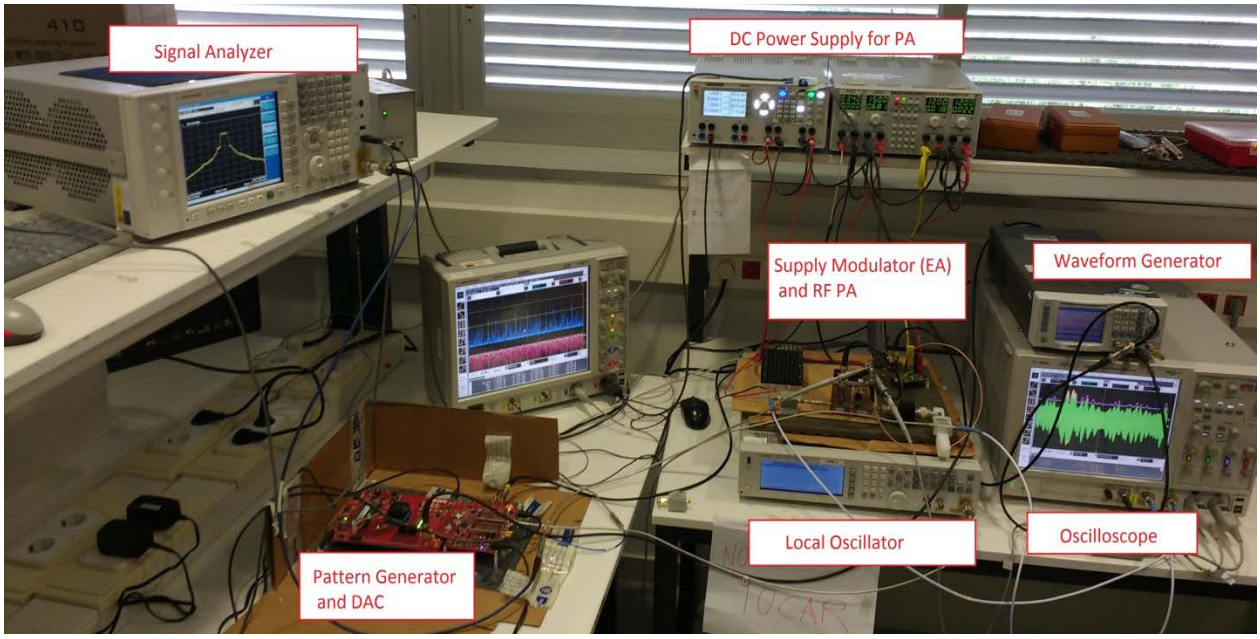

Figure 4-2: Instruments Layout

4.2 DUT Test Scenarios

The adaptive shaping algorithm discussed in 3.5.1 is tested with the hardware setup. Following section presents the test results for an LTE 5MHz signal. In view of the project objective to improve power efficiency using an envelope tracking RF PA, test scenario includes following 03 configurations.

- Dynamic Supply RF amplification without Shaping function
- Envelope Shaping using adaptive technique

- Adaptive Envelope Shaping with an additional IQ DPD block to gain further benefits in terms of linearity and reduced AM-PM distortion

A 5 MHz LTE signal is generated for testing using processing parameters defined in table 4-1. Frequency spectrum of input signal shown in fig. 4-3 shows the power distribution over the bandwidth before it is fed to envelope or signal path.

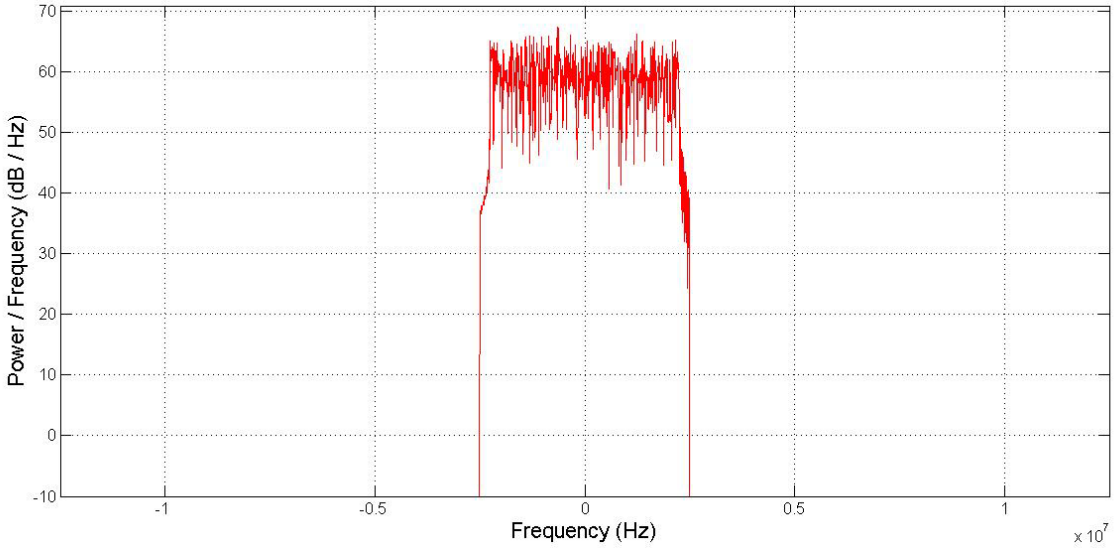

Figure 4-3: 5 MHz Input Signal Spectra

Table 4-1: Test Parameters

Parameter	Values
No. of Samples	61440
Model Type	Memory Polynomial
Local Oscillator Frequency	950 MHz
Baseband Bitrate	614.4 MHz
Lower Threshold Protection	0.4

In the sections 4.2.1 through 4.2.3 AM-AM characteristic curve, phase distortion at the output, shaping curve for supply modulation and corresponding output spectra is presented. Overall system performance will be analyzed consolidating results in section 4.3.

4.2.1 Dynamic Supply with No Shaping

Starting from a system which uses dynamic supply RF PA system based on the envelope of the input signal with a shaping block, fig. 4-4 shows an input-output amplitude response considering whole system in a black box approach. In this case, a dynamically varying voltage signal is provided to RF PA exactly following the shape of input envelope without any modification i.e. shaping function. The output curve shows nonlinearity which is a typical characteristic of RF power amplifiers. In order to linearize magnitude response, inverse distortion to the one shown in fig. 4-4 is pre-applied to the signal.

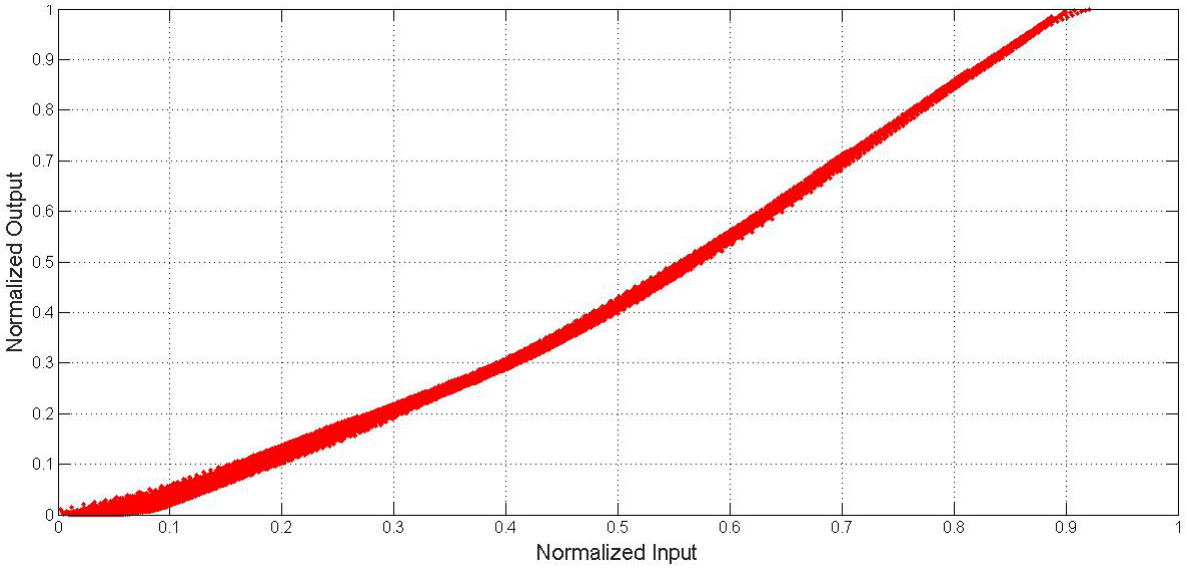

Figure 4-4: AM-AM Curve for Dynamic Supply Model without shaping function

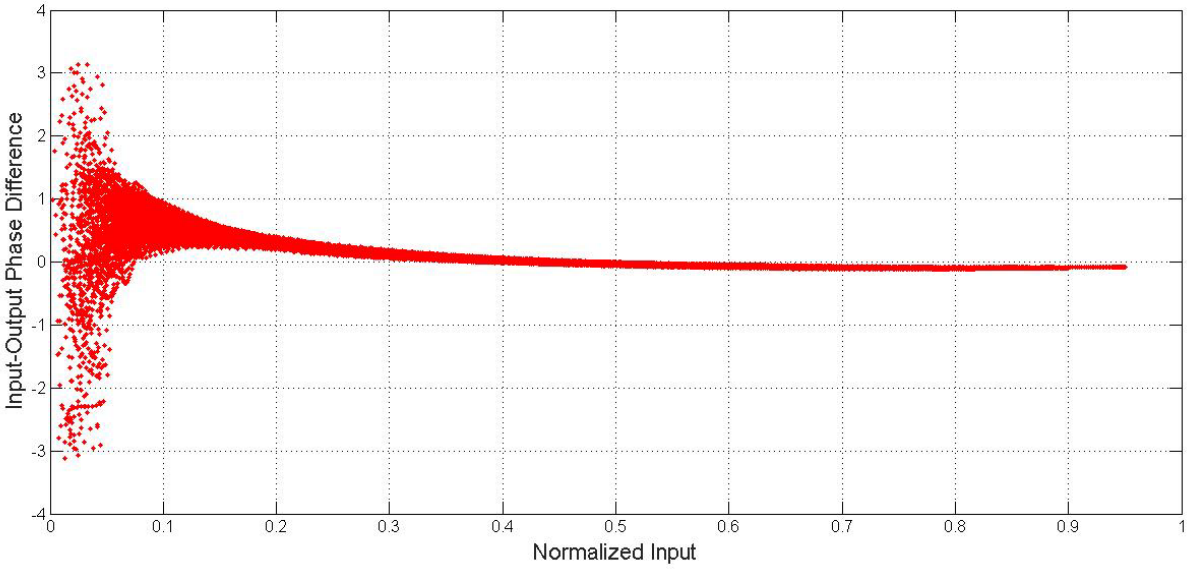

Figure 4-5: AM-PM Response for Dynamic Supply Model with shaping function

Fig. 4-5 displays phase distortion caused by RF PA at the output. AM-PM distortion removal is a significant challenge and it cannot be accomplished without the cost of added computational complexity. Fig. 4-6 presents a clearer picture on why a dynamic supply envelope tracking and shaping system performs better. Output signal frequency response of a dynamic supply system with no shaping shows a considerable amount of power leakage into sidebands. It will be compared with adaptive system in the following section.

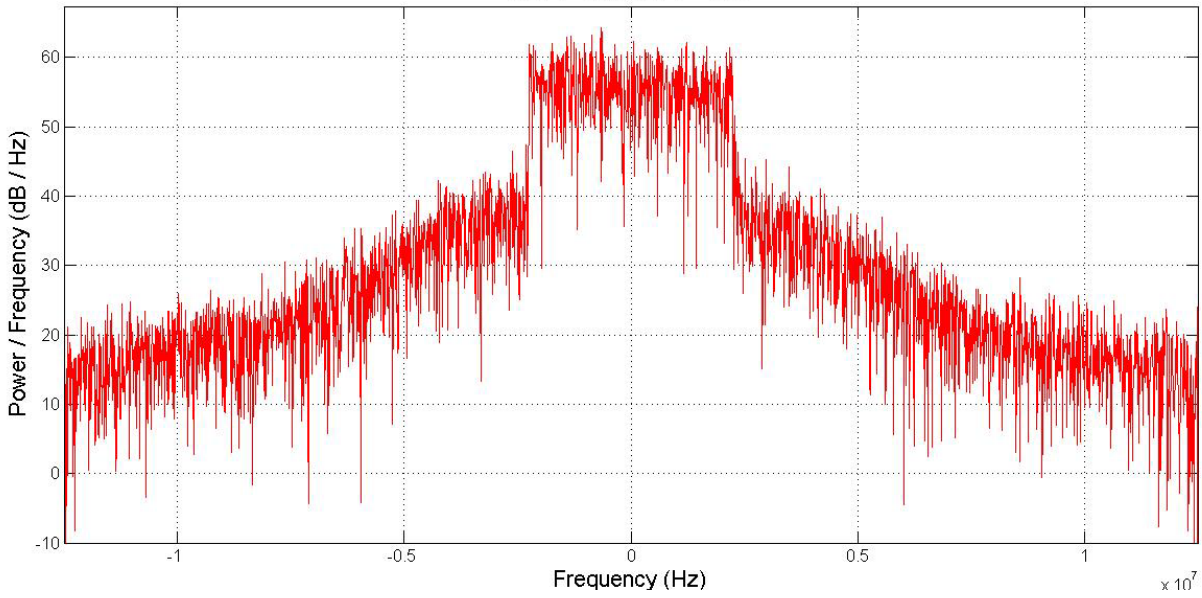

Figure 4-6: RF Output Spectrum for Dynamic Supply Model without shaping function

4.2.2 Adaptive Shaping

Adaptive shaping algorithm updates polynomial parameters used for shaping function. PA output is fed back to a shaping adaptation block which aims to minimize the error vector. Following graphs exhibit an improvement in system performance. Fig. 4-7 shows that the magnitude response of system is quite linear as compared to a no-shaping system. Contrary to the improvement in AM-AM response, the adaptive shaping algorithm does not offer much improvement in phase distortion as shown in fig. 4-8.

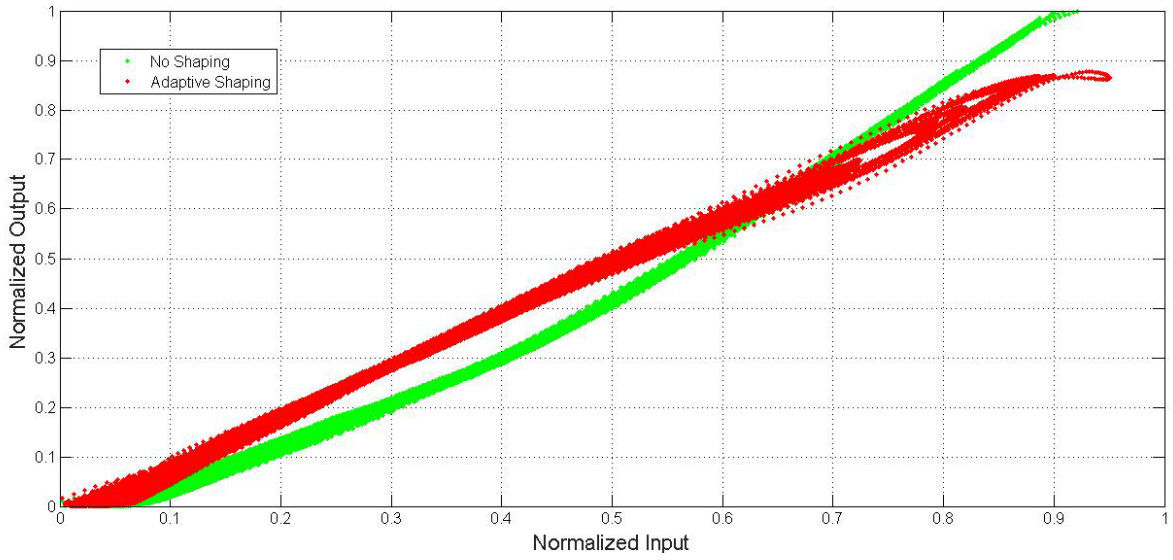

Figure 4-7: AM-AM Curve for Adaptive Shaping Model

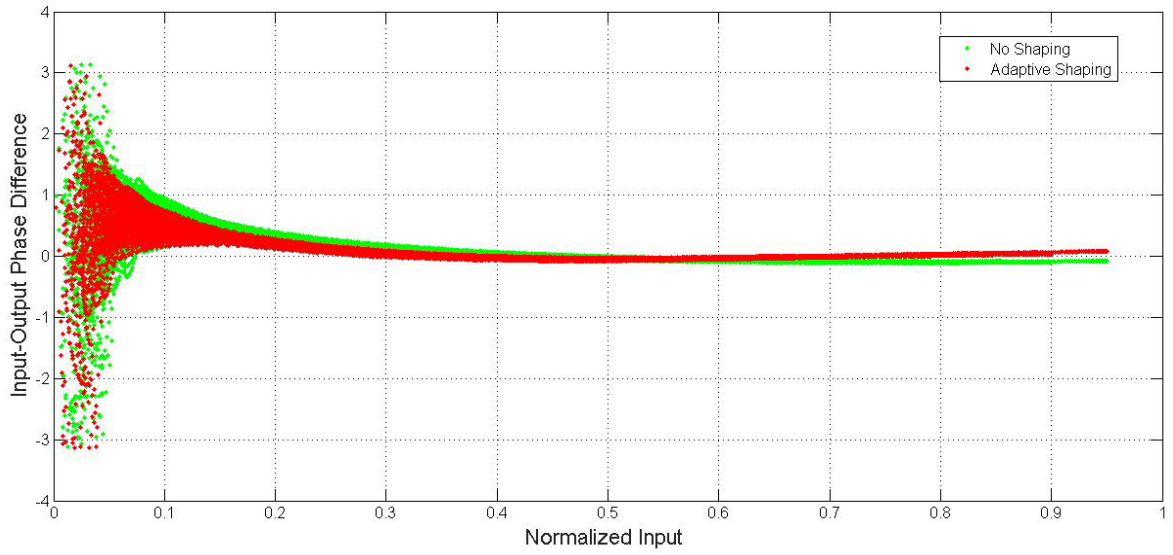

Figure 4-8: AM-PM Response for Adaptive Shaping Model

Output frequency response of adaptive shaping system (Fig. 4-9) shows that ACLR values are almost 10 dB better as compared to no-shaping approach. Although, the system operates in a linear region, the PAE is consistent due to the use of a dynamic power supply, thus highlighting the concept of optimal resource utilization.

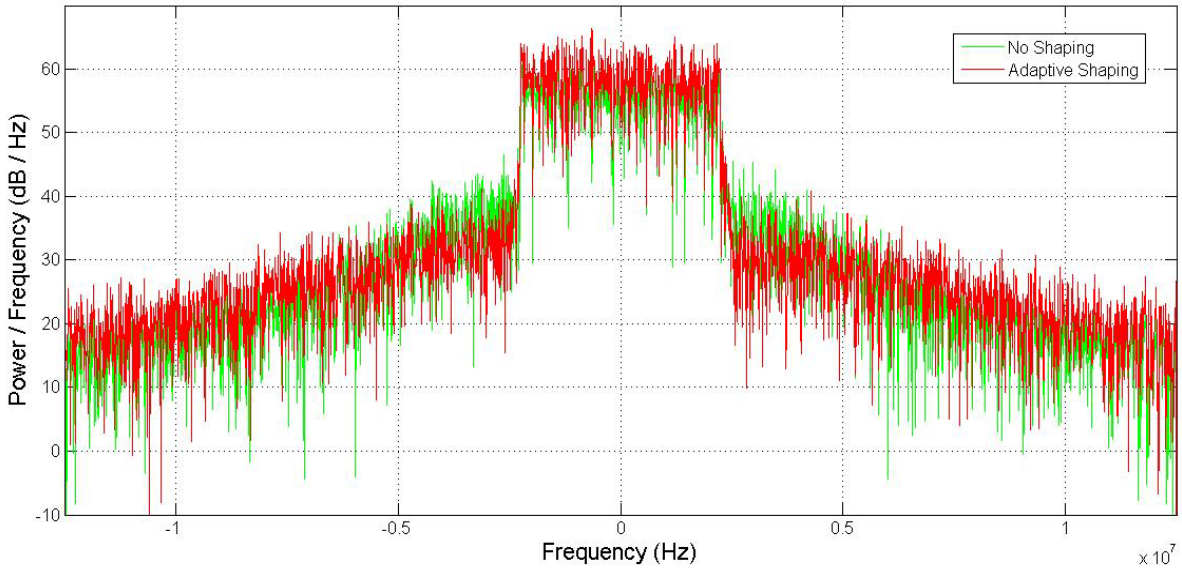

Figure 4-9: RF Output Spectrum for Adaptive Shaping Model

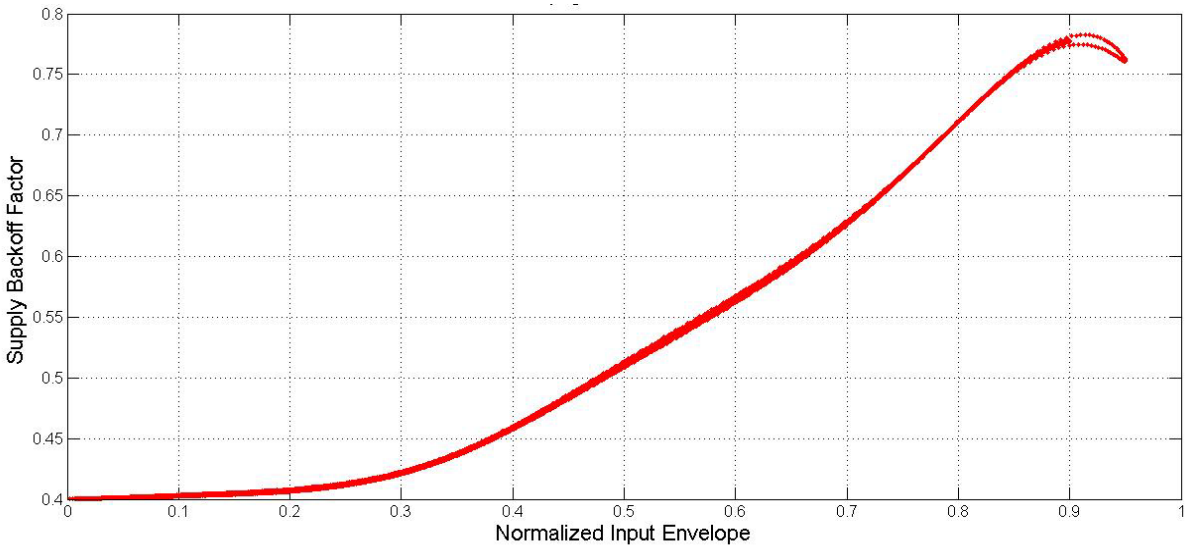

Figure 4-10: Shaping Function curve for Adaptive Shaping Model

Fig. 4-10 is the supply modulation function which yields a back-off factor value against an envelope sample and RF PA is then operated at optimum gain using that power supply.

4.2.3 Adaptive Shaping with IQ DPD

As discussed in previous chapters, phase distortion problem at the output can be overcome to some extent using further linearization process. An IQ DPD block using memory polynomial introduces an inverted estimation of RF PA output which in turn linearizes the output.

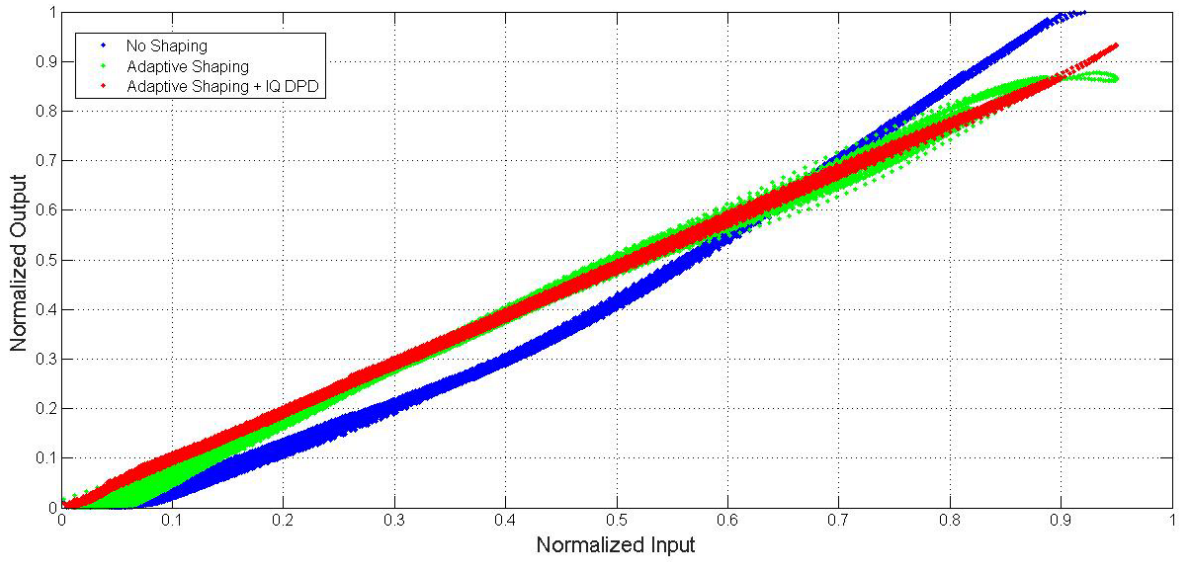

Figure 4-11: AM-AM Response for AS + IQ DPD

Introducing additional linearization techniques in signal path, improves AM-AM response (Fig. 4-11) making it virtually linear. But the actual gain is in terms of a reduced phase distortion for a complex RF signal. AM-PM response in fig. 4-12 shows a considerably less input-output phase difference as compared to no-shaping technique and adaptive shaping without an IQ DPD.

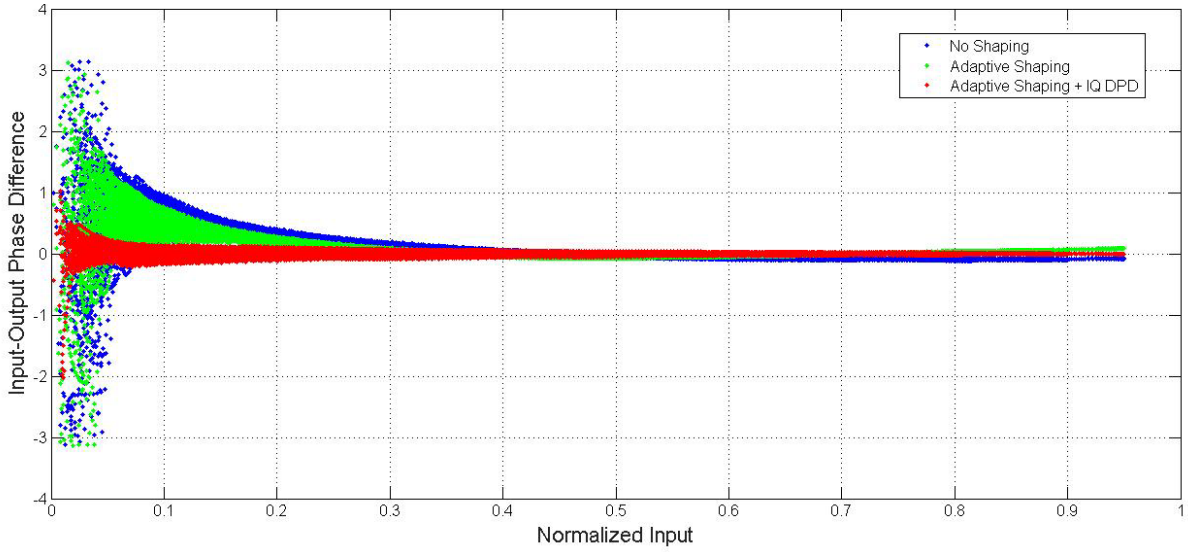

Figure 4-12: AM-PM Response for AS + IQ DPD

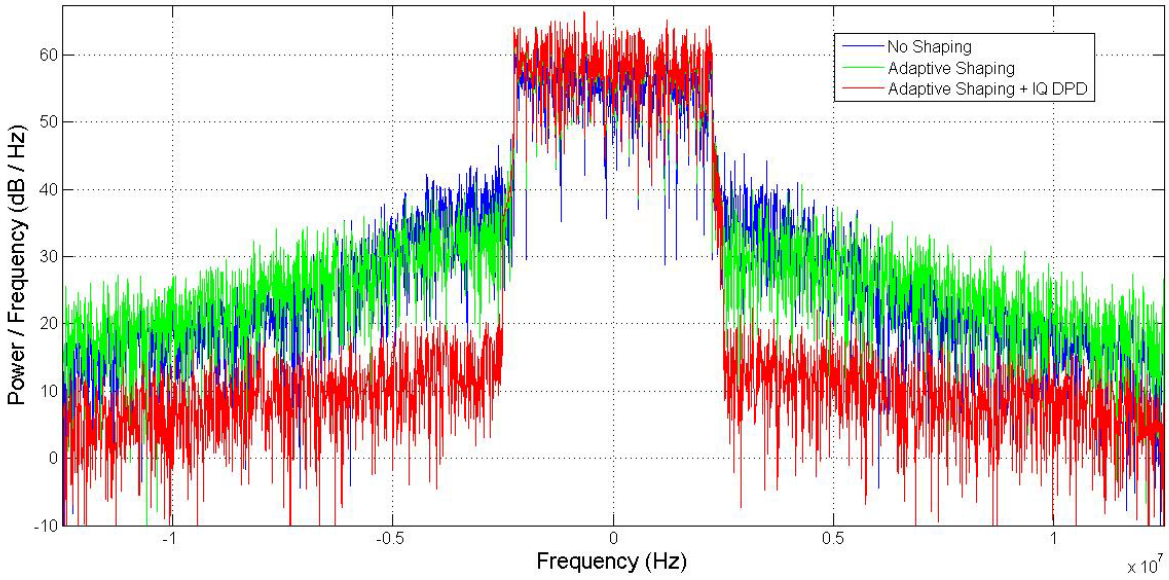

Figure 4-13: RF Output Spectrum for AS + IQ DPD

RF output spectra for test scenarios (Fig. 4-13) shows a significant ACLR improvement of 20 dB due to introduction of addition linearization of IQ DPD block. Shaping function for adaptive shaping with IQ DPD shows a linear response (Fig. 4-14). Input signal envelope is mapped to a back-off factor value to modify power supply level. Numerical values representing gradual enhancement in system performance are shown listed in table 4-2.

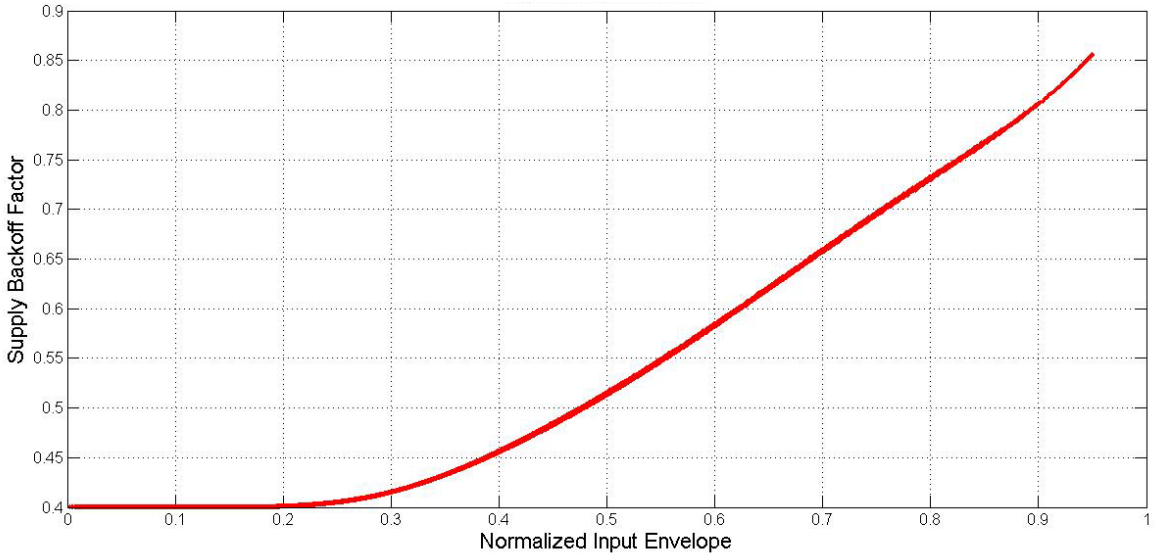

Figure 4-14: Shaping Function curve for AS + IQ DPD

4.3 Performance Comparison

To analyze system performance in terms of PAE and linearity constraints such as ACLR, values are listed in table 4-2. Taking a gradual approach, it can be seen that linearity characteristics of RF PA output improve with a compromise on PAE percentage. An ACLR improvement of 4.23 dB in lower and 5 dB in upper sideband of spectrum clearly signifies that introducing a dynamic power supply introduces performance enhancement in linearity constraints for communication standards. However, IQ DPD block with adaptive envelope shaping truly remedies the challenge of useful power leakage into sidebands. Consequently, PAE of the system improves from 42.8 % to 46.3 % but ACLR improvement of -44.55 dB and -45. 79 dB is the actual gain in terms of performance.

Table 4-2: Performance Comparison

	Linearization Scheme	**ACLR (dB)**		**NMSE (dB)**	**P_{out} (dBm)**	**PAE (%)**
		Lower	Upper			
LTE 5MHz	No Envelope Shaping	-23.10	-23.30	-17.8	27.5	49.2
	Adaptive Shaping	-27.33	-28.30	-27.4	29.7	42.8
	AS+ IQ DPD	-44.55	-45.79	-38.0	29.9	46.3

Improved value of NMSE from -27.4 dB to -38.0 defines the quality of estimation considering a black box approach. For mobile applications, a lower threshold of -38 dB is considered an acceptable solution with an output power of 26 dBm but inclusion of an IQ DPD block in signal path adds computational complexity for power constrained applications such as handheld mobile units.

4.3.1 Manual Shaping vs Adaptive Shaping

Table 4-3 lists a comparison between manual and adaptive shaping results. Manual shaping uses a pre-characterization of PA output power vs gain for different supply voltage values. As obvious from the results, overall system performance does not merit the inclusion of an

adaptive algorithm but in a real time system, static measurements of RF PA response are not feasible. Moreover, PAs based on GaN HEMT transistors exhibit soft-compression in AM-AM response when static PA characterization is performed [13]. Therefore, an adaptive algorithm which iteratively converges to an optimal shaping function is the best solution in terms of overall system performance.

Table 4-3: Manual vs Adaptive Shaping

	Linearization Scheme	ACLR (dB)		NMSE (dB)	P_{out} (dBm)	PAE (%)
		Lower	Upper			
5 MHz LTE	Adaptive Shaping	-33.00	-33.70	-27.7	33.3	47.6
	Manual Shaping	-34.2	-31.8	-26.2	33.1	51.9

4.3.2 Spline Interpolated Manual Shaping Model

Simulated results for a 5 MHz LTE signal are shown in figure 4-15 and 4-16 for 35.2667 dB and 39.267 dB gain value respectively. Equation 3.20 transforms input power in dBm to signal envelope value and corresponding power supply curve defines a back-off factor to modulate power supply.

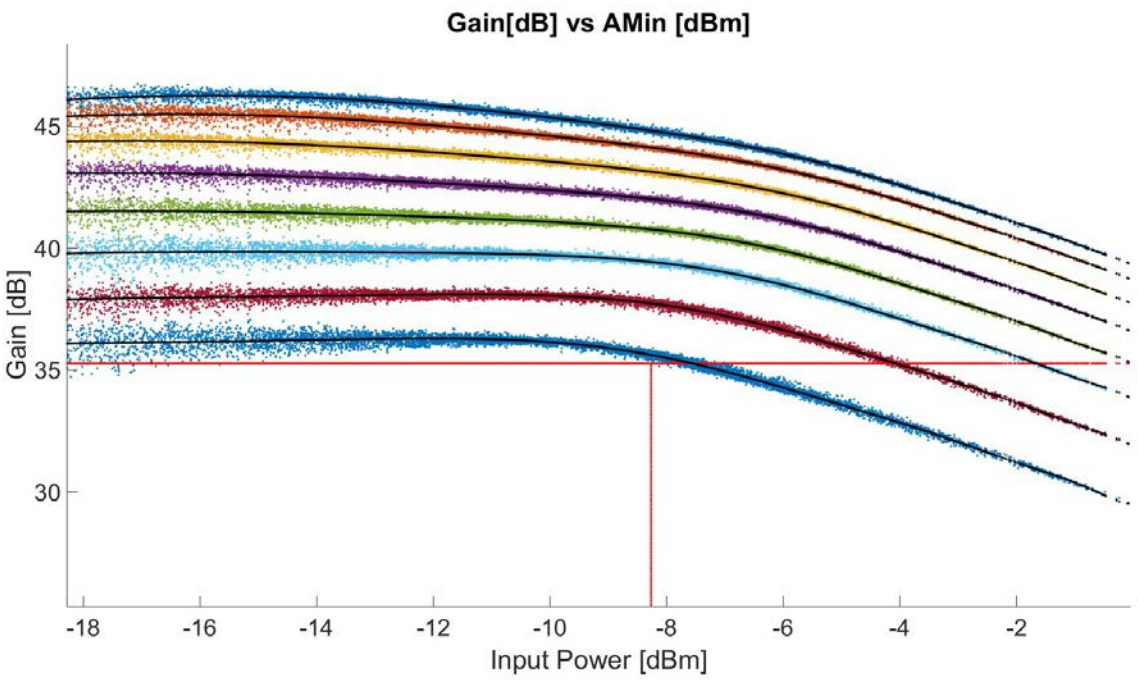

Figure 4-15: Gain vs Input Power (Targeted Gain = 35.2667dB)

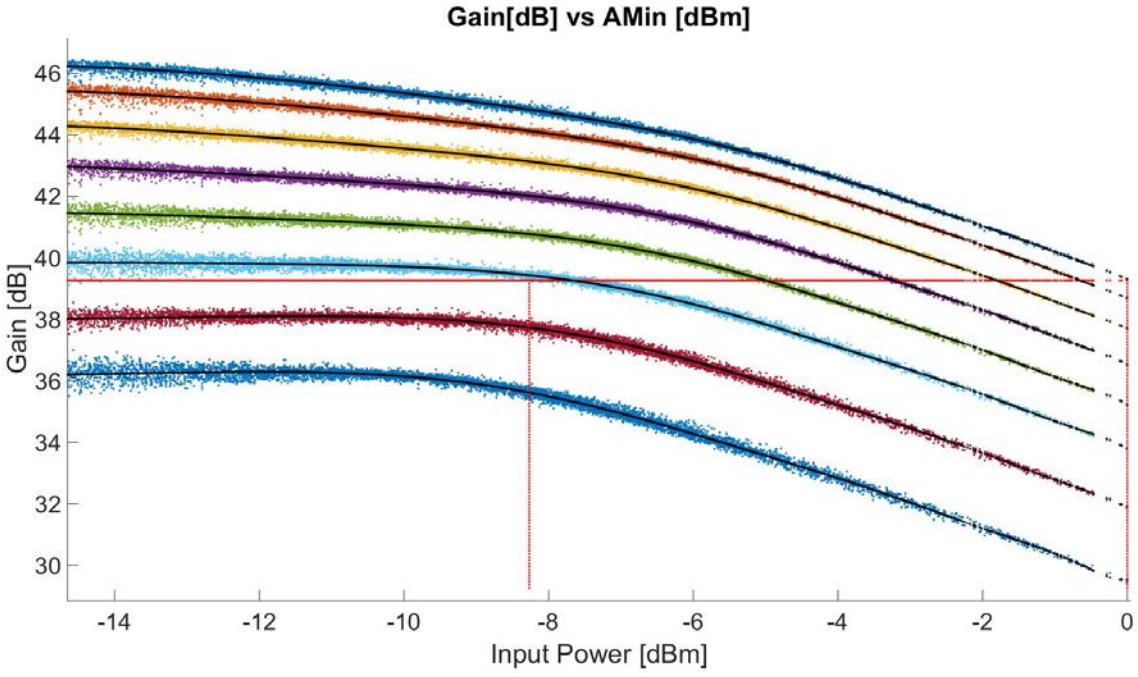

Figure 4-16: Gain vs Input Power (Targeted Gain = 39.267dB)

By manually selecting the points where the isogain line intersects the power supply curves, table 4-3 displays required supply voltage supply value. 0 dBm represents maximum input power or maximum normalized envelope value.

Table 4-4: Input Envelope and Power Supply

Targeted Gain = 35.2667dB			**Targeted Gain = 39.267dB**		
Input [dBm]	Envelope |xBB|	Supply [V]	Input [dBm]	Envelope |xBB|	Supply [V]
0	1	17.22	0	1	27.77
-1.664	0.8257	14.5	-0.666	0.9262	25.24
-4.073	0.6257	11.8	-1.807	0.8122	22.57
-7.559	0.4188	9.037	-3.247	0.6881	19.89
			-5.001	0.5623	17.22
			-7.678	0.4131	14.5

Envelope shaping function is created using data points presented in the table 4-3 with cubic spline model. Input signal envelope or magnitude is the independent variable here whereas a dynamic required value of power supply to PA is the dependent variable. Input provided to cubic spline shaping model is a 5 MHz LTE signal. Since, the system has a restraint at maximum available power supply for a certain isogain trajectory, therefore all the values of input signal envelope higher than maximum system limit are being considered to be amplified with the maximum power supply which is 17.22V for a targeted gain of 35.2667dB.

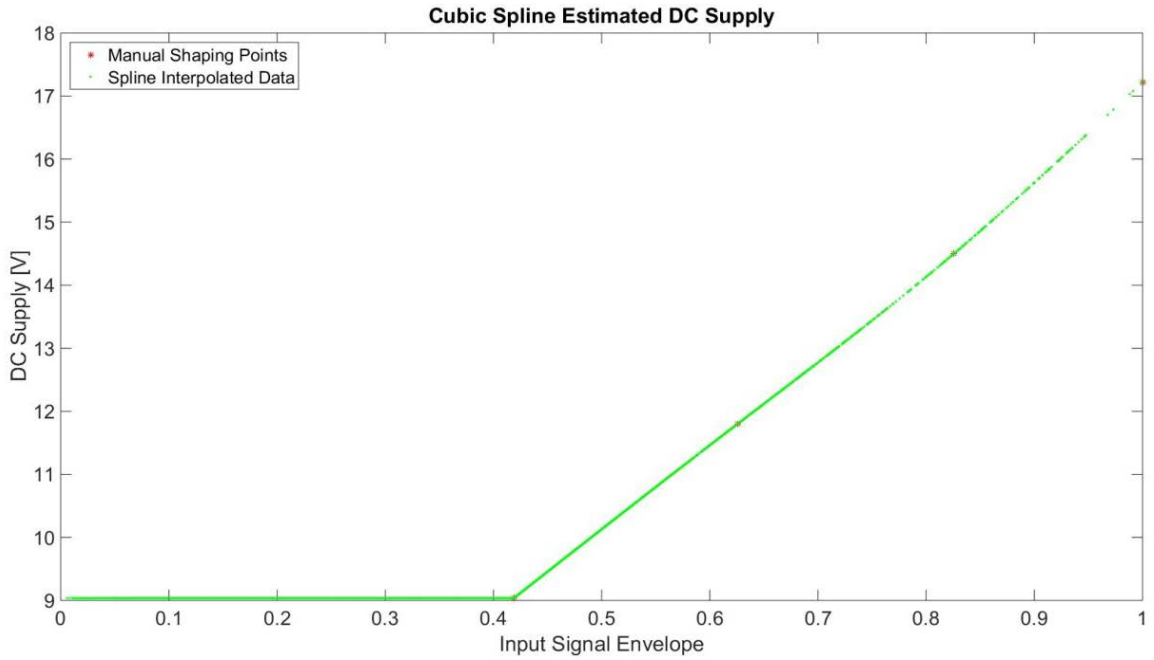

Figure 4-17: Shaping Model (35.2667dB Gain)

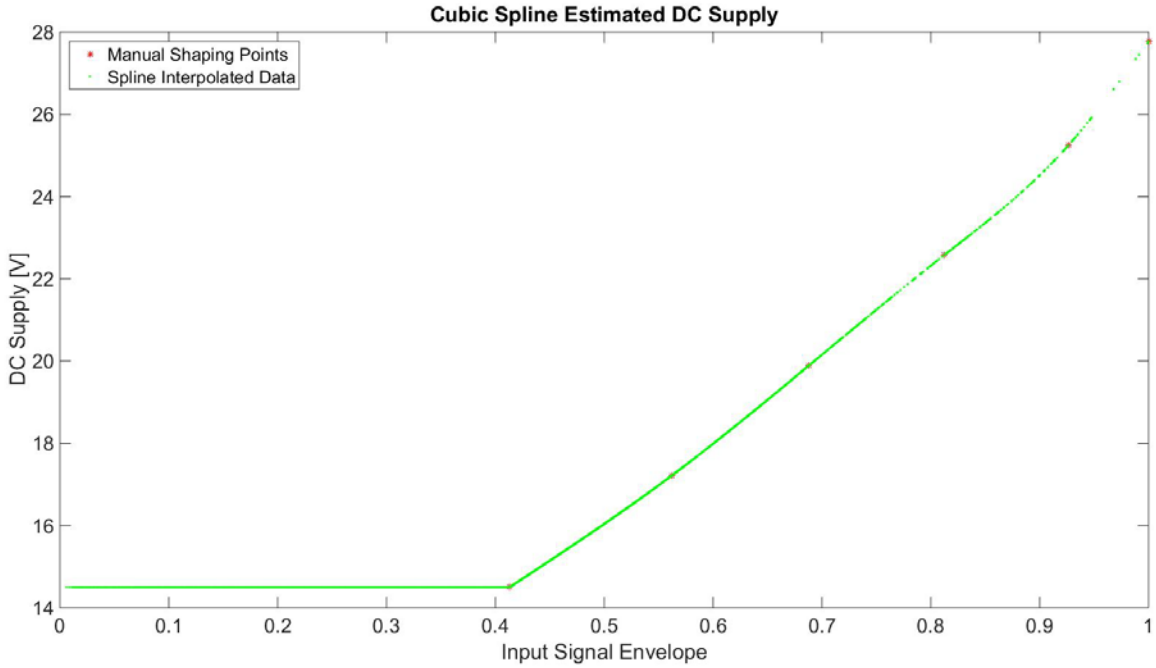

Figure 4-18: Shaping Model (39.267dB Gain)

The maximum optimal power supply at the peak of input signal envelope in shaping curve represents the system limit according to the isogain line. Meanwhile, the lower limit

corresponds to the fact that dynamic power supply cannot go as low as 0 V but has to pre-assign a threshold value of power supply to use for input with low RF power.

Cubic spline model can be incorporated into adaptive envelope shaping algorithm to replace a polynomial model to improve estimation accuracy. However, computational complexity may turn out to be a limit because unlike polynomial interpolation which uses a single function and the only controllable parameter is polynomial order or the no. of coefficients, Spline model in general uses a an independent function between each set of interpolation points. An adaptive cubic spline model in particular has to calculate 3^{rd} order equations for estimating output between 2 consecutive points and adaptation further adds to computational cost at digital signal processing stage.

5 Conclusion

Before starting to look for an alternative approach to fixed DC power supply RF PAs for high PAPR signals, it was very critical to establish a problem statement. Analysis of the performance requirements for modern communication standards lead to the idea of a dynamic supply power amplification system where only the need based power was to be consumed ideally.

After identification of the problem, basic PA principle is described linking to performance metrics for transmission quality. Along comes the need to manipulate a conventional system architecture where a modulated baseband signal is fed to an amplifier and transmitted using a fixed amount of drain supply to PA irrespective of the magnitude of the input to the system. With PA itself being a non-linear device, it has been deemed as a poor approach when the overall system resources are considered. Moreover, with the advent of various handheld devices which have limited power at their disposal, different tracking techniques for the envelope of input have offered promise.

Average power tracking and Envelope tracking improve a system's PAE. The core concept is to dynamically change which is being fed to PA as power supply based on the input signal. This variation of drain voltage is instantaneous, at sub-sample level in case of envelope tracking. With the use of envelope tracking strategy, the conventional forward path to feed baseband signal to PA divides into two paths with separate signal processing modules. Signal is fed to PA on *'Signal Path'* with an additional forward path called *'Envelope Path'* includes magnitude calculation of input signal before it controls an additional amplifier known as EA.

After gauging the system behavior and forming an input-output model, a shaping block is introduced in envelope path. Starting with a memoryless power series, the algorithm then went on to incorporate memory effect. These linearization strategies are studied, and then tested on a testbed with a DUT. The ability to test the algorithm on a hardware system has provided an insight to responses to behavioral model which are challenging to simulate on a software platform.

Shaping function in the algorithm has been based on polynomial model. A trivial alternative which saves system resources in terms of computational complexity of algorithm is to use to LUT(s). Instead of performing polynomial interpolation for each block of data, a lookup table

offer speed by pre-allocating the inputs to supply modulation circuitry. However, as established in chapter 3, Spline Interpolation can be a method which offers increased stability. For an adaptive envelope tracking and shaping block which uses a feedback from PA output, a cubic spline model may offer improvement in performance. Cubic Spline model is developed for a manual (by-hand) shaping function. Picking up a set of points from a data pool which contains input signal envelope and corresponding power supply values for an LTE 5MHz, shaping curves for different values of targeted output gain are included.

Presented in chapter 4, the results show that proposed adaptive shaping algorithm's enhances system spectral characteristics i.e. ACLR is reduced when compared to a manual shaping simulation. The results improve further when a LUT is introduced in shaping function block. The most significant improvement in overall system performance is achieved when a linearization strategy is employed for signal path as well. By introducing a DPD in signal path, the AM-PM distortion is reduced which improves system performance.

Bibliography

[1] Baker, S., "*ET101An Introduction to Envelope Tracking for RF Amplifiers,"* white paper, November 2011.

[2] The Mobile Economy Report, GSM Association, 2014.

[3] The Tauri Group, State of the Satellite Industry Report, Technical Report, Satellite Industry Association, May 2014.

[4] Jean-Didier Gayrard, Cédric Baudoin, Christine Miquel, Michel Sghedoni, *"Wireless Communications for Satellite Formation Flying,"* July 2006.

[5] Joel Vuolevi and Timo Rahknonen, "*Distortion in RF Power Amplifiers."* Artech House, 2003. ISBN:1580535399.

[6] Zhangcang Wang. *'Envelope Tracking Power Amplifiers for Wireless Communications'*. Artech House, 2014.

[7] Pere L. Gilabert, Gabriel Montoro, "*Digital Predistortion for Envelope Tracking Amplifiers,"* International Microwave Symposium, June 2013.

[8] Pere L. Gilabert, Gabriel Montoro, *"Design of Adaptive Digital Predistorter Linearizers for Envelope Tracking Power Amplifiers,"* Workshop on Signal Processing and Amplifiers 2012.

[9] Schreurs, D., M´airt´ın O'Droma, Anthony A. Goacher, Michael Gadringer, *"RF Power Amplifier Behavioral Modeling,"* The Cambridge RF and Microwave Engineering Series. Cambridge University Press, 2009. ISBN: 9780521881739.

[10] Joel Vuolevi and Timo Rahknonen. *'Distortion in RF Power Amplifiers'*. Artech House, 2003. ISBN: 1580535399.

[11] R. Neil Braithwaite. *'Principles and Design of Digital Predistortion'*. In Fa-Long Luo, editor, Digital Front End in Wireless Communications and Broadcasting—Circuits and signal Processing, chapter6. Cambridge University Press, 2011. ISBN: 9781107002135.

[12] Pedro M. Sousa, *"Digital Predistortion of Wideband Satellite Communication Signals with Reduced Observational Bandwidth and Reduced Model Order Complexity,"* MAST, UPC, Oct 2014.

[13] J. C. Pedro, L. C. Nunes, P. M. Cabral, "Soft compression and the origins of nonlinear behavior of GaN HEMTs," in Microwave Conference (EuMC), 2014 44th European, Oct 2014, pp. 1297–1300.

[14] R.Wu, Y.-T. Liu, J. Lopez, C. Schecht, Y. Li, and D. Lie, "High-Efficiency Silicon-Based Envelope-Tracking Power Amplifier Design With Envelope Shaping for Broadband

Wireless Applications," Solid-State Circuits, IEEE Journal of, vol. 48, no. 9, pp. 2030–2040, Sept 2013.

[15] D. Kim, D. Kang, J. Choi, J. Kim, Y. Cho, and B. Kim, "Optimization for Envelope Shaped Operation of Envelope Tracking Power Amplifier," Microwave Theory and Techniques, IEEE Transactions on, vol. 59, no. 7, pp. 1787–1795, July 2011.

[16] T. Rautio, H. Harju, S. Hietakangas, and T. Rahkonen, "Envelope tracking power amplifier with static predistortion linearization," Int. Journal of Circuit Theory and Applications, vol. 37, no. 2, pp. 365–375, 2009.

[17] Lucyszyn, S., "Power-Added Efficiency Errors with RF Power Amplifiers," International Journal of Electronics, Vol. 82, No. 3, March 1997, pp. 303-312.

[18] Cripps, S.C., RF Power Amplifiers for Wireless Communications, Norwood, MA: Artech House, 2006.

[19] Kim, I., et al., "High-Efficiency Hybrid EER Transmitter Using Optimized Power Amplifier," IEEE Transactions on Microwave Theory and Techniques, Vol. 56, No. 11, 2008, pp. 2582-2593.

[20] Hanington, G., et al., "High Efficiency Power Amplifier Using Dynamic Power-Supply Voltage for WCDMA Applications," IEEE Transactions on Microwave Theory and Techniques, Vol. 47, No. 8, August 1999, pp. 1471-1476.

[21] Hoversten, J.Z., M.N. Popovic, and D. Maksimovic, "Power Amifier to Envelope Modulator Interconnects for Envelope Tracking Transmitters," Intellectual property disclosure, University of Colorado at Boulder, Boulder, CO, April 2009.

[22] Aitto-oja, T., "High Efficiency Envelope Tracking Supply Voltage Modulator for High Power Base Station Amplifier Applications," 2010 IEEE MTT-S International Microwave Symposium Digest (MTT), 2010, pp.668-671.

[23] Hubbard, M., "Taming the smartphone Power Consumption Vicious Cycle," Microwave Journal, November 2012, pp. 92-96.

[24] Mike Renfro, "Programs for Natural Cubic Spline Interpolation," November 2004.

[25] Wang, K., "A Study of Cubic Spline Interpolation," Rivier Academic Journal, Vol. 9, No. 2, 2003.

[26] Huseyin Ozdemir, "Comparison of linear, cubic spline and akima interpolation methods," August 2007.